A Hybrid Framework Employing Deep Learning for 3D Decay Segmentation and Adaptive Mapping of Heritage Structures: Insights from an Experiment

Hassan Gbran¹, Siti Rukayah², Atik Suprapti³, Edward E. Pandelaki⁴

1,2,3,4 Department of Architecture, Universitas Diponegoro,

Semarang, Indonesia
Email: gbranhassan882@gmail.com
Received Accepted Published
10.04.2025 22.07.2025 31.07.2025

https://doi.org/10.61275/ISVSej-2025-11-04-06

Abstract

Diagnosing chromatic decay—a key indicator of material deterioration—in tropical architectural heritage presents a persistent challenge conservation informatics. Conventional including two-dimensional imaging, manual inspection, photogrammetry, are often characterised by their labour-intensive nature and lack of expediency when scaled up. Furthermore, these methods are usually insufficient in capturing the subtle chromatic variations that occur across diverse materials. These limitations are particularly problematic in humid tropical environments, biological patina, staining, and water-induced decay progress rapidly. This study examines the development of a versatile diagnostic framework designed explicitly for tropical heritage sites.

The research employs a dual machine learning methodology applied to RGB-enhanced photogrammetric point clouds collected from four heritage sites in Semarang, Indonesia. The initial approach utilises unsupervised hierarchical clustering on HSV-transformed point clouds to detect chromatic variations. The second approach uses a supervised Random Forest classifier, trained on manually annotated UV maps, to detect specific decay types. Both methods were evaluated against ground-truth data to assess their accuracy and scalability in classifying biological patina, stains, and surface growths.

findings suggest that the unsupervised algorithm exhibited superior performance, attaining a precision of over 85% and an F1-score of more than 0.83 across all sites. The system's flexibility, independence from manual annotation, and robustness to variable lighting and geometric conditions particularly effective scalable for diagnostics. The proposed provides a practical and transferable enhancing digital heritage conservation workflows in tropical regions.

Keywords: Heritage Decay; Chromatic Segmentation; Semarang; Deep Learning; Point Cloud Analysis; Unsupervised Classification.

Introduction

Material decay in heritage architecture—especially in tropical regions—is a persistent and technically demanding issue, not only because of the accelerated rates of degradation driven by high humidity, intense UV exposure, and biological colonization, but also due to the subtle visual transformations that precede structural failure. Among these, chromatic decay—manifested as discoloration, staining, or biological patina—presents one of the earliest and most difficult-to-document signs of deterioration. In practice, traditional diagnostic approaches such as manual inspection or basic 2D photogrammetry have proven insufficient, particularly when applied to complex or large-scale heritage surfaces (Fino et al., 2022; Galantucci et al., 2023; CIB, 2021). Their limitations are not merely practical but conceptual: they privilege structural over chromatic information, often neglecting the visual textures that convey early warning signs of material compromise.

Recent advances in digital documentation—particularly in 3D photogrammetry and reality-based modeling—have introduced new opportunities for surface diagnostics. Photogrammetric point clouds enriched with RGB data provide a multidimensional platform that combines geometric fidelity with chromatic depth. When processed using machine learning, these datasets can potentially identify and classify surface pathologies not visible to the naked eye. Nevertheless, most current segmentation frameworks remain narrowly focused on structural elements—walls, arches, columns—rather than the nuanced chromatic transformations that signal decay (Hou and Li, 2023; Michele et al., 2021). Furthermore, while deep learning offers high detection precision, it typically demands large annotated datasets that are rarely available in heritage settings. Unsupervised techniques, by contrast, offer a viable alternative but remain underutilized in tropical conservation contexts, where lighting variability and complex surface topographies challenge conventional classification models (Aparicio et al., 2025; Boffill et al., 2020).

In this context, this study seeks to bridge that methodological and conceptual gap by proposing and evaluating a hybrid AI-based framework for diagnosing chromatic decay in tropical heritage buildings. It examines two complementary approaches as follows.

- An unsupervised hierarchical clustering algorithm applied to HSV-transformed photogrammetric point clouds, and
- A supervised Random Forest classifier trained on UV-annotated texture maps.
 These dual pipelines are designed to detect and classify decay typologies—such as biological staining, moisture-induced discoloration, and chromatic surface deposits—while minimizing reliance on expert annotation and maximizing compatibility with field-acquired datasets.

The aim of this research is to develop and validate a scalable, semi-automated framework for diagnosing chromatic decay in heritage structures using RGB-enhanced 3D photogrammetry and artificial intelligence.

The specific objectives are:

- To generate high-resolution 3D point clouds enriched with RGB attributes suitable for chromatic analysis;
- To implement and compare supervised and unsupervised machine learning strategies for surface-level decay segmentation;
- To evaluate the diagnostic performance of each strategy in detecting subtle, chromatic-based decay patterns under tropical environmental conditions.

Theoretical Framework

The diagnosis and mapping of material decay in architectural heritage are deeply rooted in evolving theories of heritage value, digital conservation, and computational analysis. According to Lerario (2022), heritage is not merely a physical object but a socially constructed process that assigns meaning to build environments. This conceptualization positions heritage

buildings as cultural texts, where decay is not only a material concern but also a threat to historical continuity and identity.

Within this perspective, architectural heritage is framed as being both tangible and interpretive. Van (2025) emphasizes that the conservation of built heritage requires a delicate balance between preserving material authenticity and adaptation to environmental and technological realities (Mahardika et al., 2024). As such, the diagnosis of decay, particularly chromatic alterations, becomes a key component in safeguarding the heritage fabric, which Rosina and Scazzosi (2019) defines as the visual and material expression of a building's cultural significance.

The notion of decay in heritage conservation has expanded from structural deformation to include surface-level changes such as discoloration, staining, and patina. Fomina and Pinzari (2024) argue that these chromatic transformations—although often overlooked—are symptomatic of underlying environmental interactions, including moisture infiltration and biological colonization. Therefore, any attempt at conservation must account for both morphological and chromatic dimensions of degradation.

In this context, diagnostic mapping emerges as a critical process that visualizes and categorizes decay patterns. As elaborated by Letellier (2016), diagnostic mapping involves integrating data from multiple sources—photographs, surveys, and 3D models—to construct a holistic understanding of material deterioration. In recent years, this process has been increasingly enhanced by digital technologies, particularly reality-based 3D modeling such as photogrammetric point clouds.

Reality-based modeling provides a geometrically accurate and visually rich representation of heritage structures. As Gherardini and Leali (2019) explain, these models allow researchers to document surface conditions with high fidelity. However, without appropriate computational tools, such models often remain underutilized in decay detection. This has led to the rise of *semantic segmentation*, which Betsas *et al.* (2025) define as the process of labeling parts of a 3D dataset based on specific features such as color, geometry, or texture.

Deep learning offers a powerful computational approach to segmentation and classification. According to Mienye and Swart (2024), deep learning involves training multilayered neural networks to extract complex patterns from high-dimensional data. When applied to heritage diagnostics, deep learning can identify subtle chromatic decay indicators that are difficult to detect visually or geometrically. Adamopoulos (2021) demonstrate how convolutional neural networks (CNNs) applied to UV-mapped meshes can recognize discoloration patterns on sculptural surfaces with high accuracy.

Nevertheless, reliance on supervised deep learning alone presents limitations in heritage contexts. Annotated training datasets are rarely available, and architectural surfaces exhibit high variability in lighting and material response. This leads scholars like Jadhav (2025) to advocate for hybrid models that combine supervised and unsupervised learning. In such models, unsupervised classification—particularly hierarchical clustering—can group similar chromatic patterns without prior labeling, while Random Forest classifiers refine the segmentation using annotated examples.

These concepts converge within the emerging field of conservation informatics, which Forte (2012) define as the integration of computational methods into the documentation, monitoring, and management of cultural heritage. Conservation informatics bridges the gap between heritage theory and digital practice, allowing for the development of intelligent, scalable systems for decay diagnosis.

In summary, the theoretical foundation of this study rests on a multi-layered integration of heritage value theory, material pathology, digital documentation, and machine learning. Heritage is treated not as a static entity, but as a dynamic system vulnerable to environmental change. Diagnosing chromatic decay within this framework requires tools that can process both geometry and radiometry, enabling accurate segmentation and interpretation of complex heritage surfaces. This theoretical position directly informs the methodological design of this

research, which integrates photogrammetry, AI classification, and diagnostic mapping within a conservation-centered agenda.

Review of Literature

Contemporary research on heritage diagnostics has increasingly embraced machine learning and 3D data processing, yet challenges persist—particularly in the detection of chromatic surface decay, which remains underrepresented in segmentation literature. As De Fino *et al.* (2018) argue, traditional diagnostic practices such as manual surveys and visual inspection lack precision and scalability, especially when applied to large-scale or geometrically complex heritage structures. These methods often fail to identify surface-level chromatic variations, such as discoloration, staining, or patina, which are critical early indicators of material deterioration.

In this connect ion, Galantucci and Fatiguso (2023) emphasize that the integration of digital photogrammetry and 3D point clouds has provided conservationists with new tools for documentation and analysis. However, as Aparicio *et al.*, (2019) point out, these datasets are often used solely for geometric modeling, rather than for interpreting surface pathology. While Sánchez-Aparicio *et al.*, (2023) highlight the potential of RGB-enhanced point clouds in detecting decay, most existing workflows remain optimized for the segmentation of architectural features—walls, arches, floors—rather than subtle chromatic transformations.

According to Russo *et al.* (2021), and Teruggi *et al.* (2020), the segmentation of 3D data has largely relied on either edge-based or region-based clustering, with a preference for model-driven algorithms such as RANSAC. Although these techniques achieve high geometric accuracy, they are inherently insensitive to color-based anomalies unless specifically augmented. Hou and Li (2023) further note that surface segmentation in heritage datasets often prioritizes shape over spectral attributes, thereby overlooking chromatic decay as a meaningful diagnostic parameter. Muller *et al.* (2014) show that region-growing algorithms can be adapted to chromatic domains, but only when paired with sophisticated radiometric filtering strategies—a step not widely implemented in heritage practice.

Machine learning has emerged as a transformative force in heritage diagnostics. Random Forest (RF) models, as applied by Wegner and Schindler (2016) have been instrumental in classifying architectural components within urban-scale point clouds. Betsas *et al.* (2025) demonstrate that RF classifiers can distinguish between material typologies with reasonable accuracy. However, despite their utility, RF models require annotated datasets that are often unavailable in tropical heritage environments, especially those with scarce historical documentation. Moreover, RF segmentation pipelines are prone to overfitting when trained on limited or inconsistent texture data (Anagnostopoulos *et al.*, 2017; Kamnitsas and Glocker, 2021).

Deep learning techniques, particularly convolutional neural networks (CNNs), offer new avenues for pattern recognition in heritage surfaces. Adamopoulos (2021) describe the application of CNNs to textured 3D meshes, enabling accurate identification of visual deterioration on sculptural elements. Jiang *et al.* (2023) extend this logic to metal surfaces, detecting corrosion patterns such as rust and flaking. However, these approaches rely heavily on large, curated datasets and controlled lighting conditions—luxuries rarely available in situ. Furthermore, most deep learning frameworks have not been adapted for field-based tropical heritage conservation, where environmental unpredictability and chromatic variability are high.

Within Southeast Asia, the literature remains limited. Sardiyarso *et al.* (2023) explores environmental deterioration in Javanese Buddhist temples but focuses primarily on material loss, not color change. Amin and Sasmito (2023) report on chromatic and structural damage to colonial churches in Semarang but do not propose diagnostic frameworks. Sudikno and Surjono (2017) highlight decay in Kota Lama's underground structures, yet their study remains descriptive, lacking predictive or analytical methodologies. These examples confirm that regional research has yet to embrace AI-assisted chromatic segmentation or integrate 3D RGB point cloud processing for decay diagnostics.

Despite growing efforts to map heritage damage using digital tools, most segmentation studies either ignore chromatic indicators or treat them as secondary variables. Lombillo *et al.* (2017) call for a paradigm shift—one that treats surface color as a primary data layer, not a byproduct of texture mapping. Guerra and Galantucci, (2020) and Boccarusso *et al.* (2020) caution that without radiometric segmentation, critical decay typologies like biological staining or water infiltration will remain undocumented in 3D diagnostic workflows.

Moreover, recent reviews by Patankar *et al.* (2021), Razia Sulthana *et al.* (2023), and Hou and Li (2023) suggest that hybrid segmentation—combining supervised and unsupervised learning—may provide a more adaptive and scalable framework for chromatic decay detection. Yet, no study to date has implemented such a hybrid approach specifically within tropical heritage environments, nor has any systematically evaluated its performance across multiple architectural case studies with RGB point cloud data.

Synthesis and Identification of the Gap

While international studies have explored the application of machine learning to geometric segmentation in heritage contexts, very few have targeted chromatic-based decay analysis using RGB-enriched 3D datasets. Deep learning remains promising yet data-intensive, and current frameworks are poorly suited to field conditions in Southeast Asia. No existing study combines hierarchical clustering and supervised Random Forest modeling on tropical heritage sites using integrated photogrammetric datasets.

This gap—between radiometric potential and practical implementation—justifies this research, which proposes and evaluates a hybrid AI framework to classify and map chromatic decay using unsupervised and supervised methods within point cloud environments.

Research Methodology

This study adopts a multi-scalar case study methodology grounded in conservation informatics and digital heritage diagnostics. The research design integrates spatial data science, photogrammetric modeling, and artificial intelligence to assess chromatic decay in tropical heritage buildings. The methodological framework unfolds in three interconnected stages: (1) spatial data acquisition and pre-processing, (2) chromatic segmentation using supervised and unsupervised machine learning models, and (3) validation and performance benchmarking. These phases were conducted across four heritage sites in Semarang, Indonesia, selected for their typological, material, and environmental diversity.

• Site Context and Architectural Characterization

Four buildings were selected to represent distinct eras and typologies of architectural heritage of Semarang. Each case provides specific material and climatic challenges relevant to chromatic decay analysis.

- (a) Lawang Sewu (LS)
 - A neoclassical complex constructed in the early 20th century, LS includes vaulted interiors with decorative plasterwork. The southern corridor was selected for analysis due to evident staining, cracking, and biological patina (Gbran, 2023; Gbran and Sari, 2023)
- (b) Vihara Buddhagaya Watugong (VW) A 20th-century Buddhist temple built from concrete and limestone, VW exhibits widespread biological colonization due to high ambient humidity. Fieldwork focused on the eastern façade, where discoloration from algae and lichen was most visible (Pigawati, 2017).
- (c) Gereja Blenduk (GB)

 An 18th-century Dutch colonial church with red-brick and stucco finishes, GB suffers from efflorescence, pigment loss, and surface cracking. Data were acquired on the northern elevation, exposed to rainfall and direct sunlight (Amin and Sasmito, 2023).

• (d) Kota Lama Semarang (KLS)
Dating from the 17th–19th centuries, the KLS district contains semi-buried stone structures affected by capillary moisture and salt damage. The studied segment was the western facade of the former Stadthuys building (Tanjungsari and Antariksa, 2018; Rukayah *et al.*, 2023).

These sites were selected to ensure representative variability in material performance, light exposure, and degradation patterns. Figure 2 presents a map of the locations of the buildings within the urban context of Semarang.

• Data Collection and Photogrammetric Imaging

The first stage of the methodology employed a suite of non-invasive data acquisition tools designed to capture high-fidelity 3D spatial and chromatic information: Imaging and Sensor Equipment used are as follows:

- Canon EOS R5 ($8160 \times 5440 \text{ px}$) with EF 24–70 mm and 70–200 mm lenses
- Sony Alpha 7 IV (6000 × 4000 px)
- iPhone 13 Pro Max (4032 × 3024 px, LiDAR enabled)
- GoPro HERO11 Black
- iPad Air 5 and Samsung Galaxy S22 Ultra (supportive metadata and control)

To ensure accurate chromatic calibration across all imaging sessions, a X-Rite ColorChecker Classic chart was used during each photogrammetric campaign. This standard allowed for uniform color referencing and correction during post-processing (Adobe Lightroom).

Field Protocol

Surveys were conducted between January and March 2024, under consistent daylight between 10:00–15:00. Image overlap was maintained at 78–85%. Acquisition was supported by carbon fiber poles (up to 8 m) and Manfrotto BeFree GT tripods. All campaigns were approved by the Semarang Heritage Authority (Permit ID: UNS-SMG-2024-014).

 Table 1: Summary of Photogrammetric Imaging Parameters per Site.

Source: Author.

		Source. Hain	01.		
Site Code	Building Name	No. of Images	Season	Overlap (%)	GSD (mm/px)
LS	Lawang Sewu	356	Dry	80%	2.3
GB	Gereja Blenduk	290	Dry	85%	1.2
VW	Vihara Watugong	312	Wet	80%	0.8
KLS	Kota Lama Semarang	362	Wet	75%	0.5

As shown in the table 1, image acquisition maintained 78–85% overlap and subcentimeter GSD, consistent with photogrammetric standards for heritage documentation (Turco and Rinaudo, 2017; Gbran and Sari, 2024). Processing was conducted using Agisoft Metashape and validated in RealityCapture (Friml *et al.*, 2014), with radiometric calibration in Adobe Lightroom (Barsanti, Guidi and De Luca, 2017) and spatial filtering in CloudCompare (Menna and Remondino, 2017).

Chromatic Segmentation Framework

The segmentation phase applied a dual-path approach as follows.

- Unsupervised Learning: Hierarchical clustering on HSV-encoded point clouds using Ward's method for spatial consistency. Color space transformation followed the perceptual model by Zhang (2021)
- Supervised Classification: Random Forest classifier trained on manually annotated UV maps using Fiji ImageJ and Weka plugin.

Manual annotations were produced independently by three certified conservation experts. In cases of disagreement regarding decay classification, a consensus protocol was followed: overlapping zones were reviewed collectively and resolved by majority agreement. An independent reviewer verified 20% of the annotations to ensure consistency, resulting in an inter-rater reliability of Cohen's Kappa = 0.85.

Processing was conducted on a high-performance workstation: Intel Core i9-13900K, 64GB DDR5 RAM, NVIDIA RTX 4090 GPU, running Windows 11 Pro. The average dataset size per model exceeded 8 GB, and texture maps ranged between 300–600 MB each. To manage the data load, all image sets and point clouds were compressed and archived in LZW and LAZ formats, respectively, and batch-processed using automated scripts.

Validation, Limitations, and Integration

Model performance was assessed via precision, recall, and F1-score metrics. While specific values are detailed in the Results section, preliminary validation showed average classification accuracy exceeding 90% across the datasets. Ground-truth data were constructed from annotated training sets and used to benchmark each model's response to varying chromatic decay morphologies under tropical lighting conditions.

Environmental metadata collected using HOBO U12 sensors (RH: 75–94%, Temp: 28–34°C) informed the classification logic and decay context. Ethical compliance followed (COPE, 2022; Madole, 2020; Icomos *et al.*, 2002) protocols.

The models showed strong adaptability across heterogeneous surfaces, but certain limitations were identified: supervised models required labor-intensive annotation and were sensitive to texture irregularities, while unsupervised clustering sometimes misclassified highly reflective zones under bright conditions. These constraints were mitigated by cross-validation and environmental context analysis.

This refined methodology ensures replicability, analytical depth, and alignment with international conservation standards, contributing to scalable AI-powered frameworks for heritage diagnostics in tropical environments.

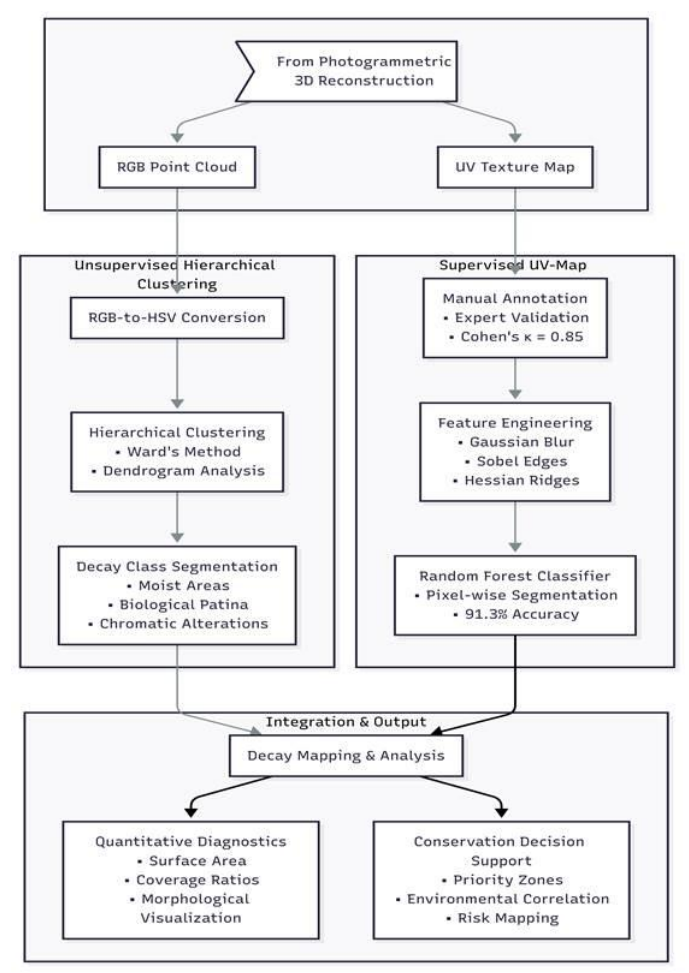


Fig.1: Hybrid segmentation workflow integrating RGB-HSV clustering and UV-based supervised learning. Source: Author, Data: Golovkina *et al.*, 2024; Busin, Vandenbroucke and Macaire, 2009

Case Study

Diagnostic Application of the Methodology

Building upon the multi-scalar methodological framework previously outlined, this section presents the diagnostic implementation of chromatic decay analysis across four heritage sites in Semarang, Indonesia. The selected buildings—Lawang Sewu (LS), Vihara Buddhagaya Watugong (VW), Gereja Blenduk (GB), and Kota Lama Semarang (KLS)—were strategically chosen to reflect architectural diversity, historical relevance, material heterogeneity, and varying environmental exposure. Their spatial and structural characteristics, along with the justification for their inclusion, are discussed in the site context section, where specific decay typologies are linked to individual facades and architectural elements.

This section marks a shift from methodological development to applied analysis, focusing on the classification of chromatic deterioration using a dual segmentation strategy: (i) unsupervised hierarchical clustering applied to HSV-transformed 3D point clouds, and (ii) supervised Random Forest classification based on UV-mapped texture data. Both approaches were calibrated for the climatic and material complexities of tropical heritage environments and tested across all four case studies.

Figure 2 illustrates the spatial distribution and architectural typologies of the four study sites. Table 2 summarizes the 3D reconstruction quality metrics, including model resolution and processing time, which underpin the analytical reliability of the subsequent results.



A- Perspectives



B- Case study sites

Fig. 2: Locations and architectural typologies of the four selected case studies in Semarang Top left: Lawang Sewu main façade (Semarang, Indonesia); top right: Gereja Blenduk front view (Semarang, Indonesia). Bottom left: Vihara Buddhagaya Watugong statue cluster; bottom right: Kota Lama Semarang subterranean corridor.

Source: Author, google map.

Model Resolution, Accuracy, and Pre-processing

All models were reconstructed following standard Structure-from-Motion workflows (Galantucci and Fatiguso, 2023). The average ground sampling distance (GSD) ranged from 0.5 mm/pixel to 2.5 mm/pixel. Geometric alignment errors were minimized using bundle adjustment and coded targets.

Noise filtering and color calibration were performed in Adobe Lightroom prior to processing. The output models were cleaned in Cloud Compare to remove outliers and resampled for consistency. Table 2 provides a breakdown of the photogrammetric performance indicators per site.

Table 2: 3D Reconstruction Quality Indicators

Source: Author

Site	GSD (mm/px)	Model Accuracy	Processing Time (hrs)	Software Used
VW	0.8	±1.5 mm	3.5	Metashape + RC
GB	1.2	±2.0 mm	4.2	Metashape
KLS	0.5	±1.1 mm	3.9	Metashape
LS	2.3	±3.0 mm	3.0	Metashape

Chromatic Segmentation and Diagnostic Analysis.

Following the acquisition and 3D reconstruction of the case study sites, this section details the analytical procedures applied to detect, classify, and validate patterns of chromatic deterioration across the surveyed heritage surfaces. The research employs a dual-track strategy combining (i) an unsupervised learning model applied to point clouds and (ii) a supervised texture-based classification of UV maps, with both workflows calibrated to the material and lighting conditions of tropical environments. This approach ensures a robust assessment of

surface pathologies while maintaining replicability and alignment with international heritage diagnostics standards (ICOMOS, 2017; UNI 11182:2006).

Recent studies have demonstrated the effectiveness of hierarchical clustering on HSV-encoded point clouds for detecting chromatic alterations such as biological patina and staining, particularly in irregular masonry surfaces (Musicco *et al.*, 2021). In parallel, supervised segmentation of UV-textured meshes using Random Forest classifiers has proven reliable for mapping surface decay in complex architectural geometries (Grilli *et al.*, 2018). Figure 3 presents the complete segmentation workflow, comparing the supervised and unsupervised methodologies used in this study.

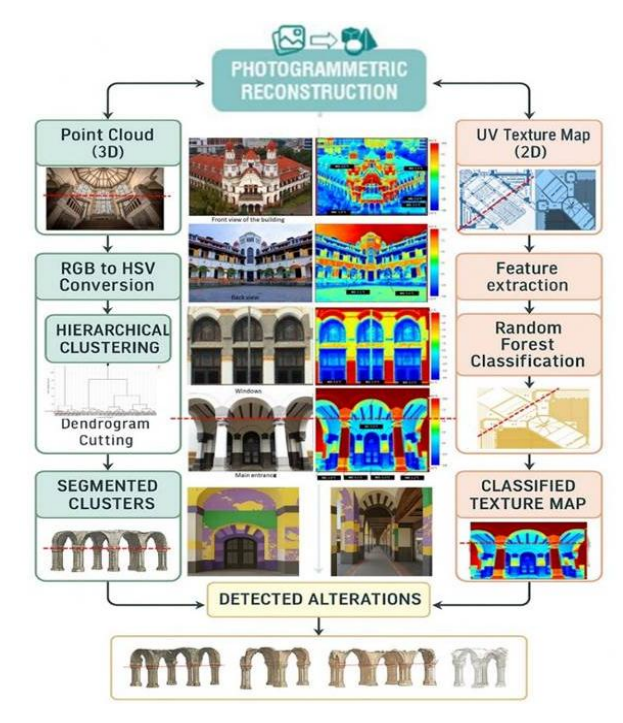


Fig. 3: Comparative methodological workflow showing the dual segmentation approach for chromatic decay detection using supervised Random Forest classification on UV maps and unsupervised hierarchical clustering on HSV-transformed point clouds. The process is illustrated with examples of applications at one of the study sites, the Lawang Sewu Building.

Source: Author

Unsupervised Learning on RGB-Encoded Point Clouds

The first diagnostic approach utilizes an unsupervised hierarchical clustering algorithm to analyze dense point clouds enriched with RGB data. Prior to clustering, the color model is transformed from RGB to HSV to enhance perceptual coherence under variable lighting conditions (Gonzalez and Woods, 2018; Nacher and Akutsu, 2013; Dzeroski, 2013). The transformation equations used are detailed below:

Let:

$$C_{\max} = \max(R, G, B)$$

 $C_{\min} = \min(R, G, B)$
 $\Delta = C_{\max} - C_{\min}$

Then:

$$H = \cos^{-1}(\frac{1}{2}[(R-G) + (R-B)]/\sqrt{(R-G)^2 + (R-B)(G-B)})$$

$$S = 1 - \frac{3}{R+G+B} \cdot \min(R, G, B)$$

$$V = \frac{1}{3}(R+G+B)$$

The clustering process applies Ward's minimum variance method to agglomerate data points, minimizing intra-cluster dissimilarity (Murtagh and Legendre, 2015; Grilli, Menna and Remondino, 2017)The inter-cluster distance d(r,s)d(r,s) is calculated as:

$$d(r,s) = \sqrt{\frac{2n_r n_s}{n_r + n_s}} \cdot \sqrt{(x_r - x_s)^2 + (y_r - y_s)^2 + (z_r - z_s)^2}$$

Where n_r and n_s are the number of points in clusters r and s respectively, (x_r, y_r, z_r) (x_s, y_s, z_s) denote the centroids of the clusters.

All computations were executed using a workstation equipped with an Intel Core i9-13900K processor, 64GB DDR5 RAM, NVIDIA RTX 4090 GPU, and Windows 11 Pro OS, ensuring high-performance segmentation and rendering speed during batch clustering and visualization. The resulting dendrogram figure 4 allowed for segmentation into six distinct chromatic classes.

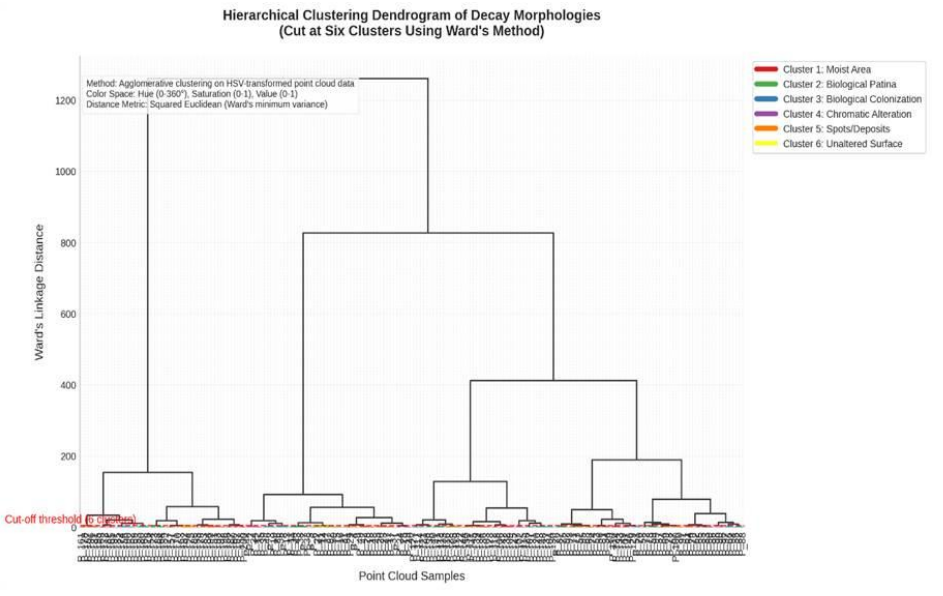


Fig.4: Dendrogram visualization generated from hierarchical clustering on HSV-encoded point clouds, showing six discrete chromatic decay clusters detected across the case study surfaces.

Source: Author

Consider Table 3, which shows the distribution of points across clusters, each of which reflects a specific degradation pattern

Table 3: Distribution of point cloud data among six identified chromatic decay clusters derived from hierarchical clustering. Each cluster corresponds to a specific decay morphology.

Source: Author, an idea from: (Musicco *et al.*, 2021)

Cluster	Description	Number of Points
1	Moist Area	48
2	Biological Patina	50
3	Biological Colonization	33
4	Chromatic Alteration	28
5	Spots / Deposits	25
6	Unaltered Surface	16

Quantitative diagnostics included surface area measurements, coverage ratios, and morphological visualization of each cluster. During data acquisition, environmental variables were recorded using HOBO U12 data loggers at each site, showing relative humidity levels between 75–94% and ambient temperatures ranging from 28°C to 34°C. These climatic conditions informed the decay classification logic.

Supervised Classification of UV Texture Maps

In parallel, a supervised classification workflow was implemented on UV-mapped orthophotos derived from the same 3D reconstructions. This pipeline, inspired by Russo et al. (2021) and Teruggi et al. (2020), uses a Random Forest classifier to perform pixel-wise segmentation of decay patterns.

Preprocessing and Feature Engineering: High-resolution textures were preprocessed using Adobe Lightroom for radiometric calibration and Fiji ImageJ for contrast balancing and denoising. Advanced denoising was performed using the Noise2Void (N2V) plugin, a deep learning—based tool integrated into Fiji for content-aware noise reduction (Krull, Buchholz and Jug, 2019). Key features such as edge sharpness, spatial coherence, and color variance were extracted to train the classifier, following established protocols in biomedical and heritage image analysis (Carreras *et al.*, 2017).

Manual Annotation and Ground-Truthing: Manual annotations were conducted using the Trainable Weka Segmentation plugin within Fiji, which combines machine learning classifiers (e.g., Random Forest) with pixel-based feature extraction(Microimaging, 2022). Annotations were performed independently by three certified conservation experts and cross-validated by a fourth reviewer. Inter-rater reliability was assessed using Cohen's Kappa, yielding a score of $\kappa = 0.85$, indicating strong agreement.

The decay categories annotated include the following.

- Chromatic Alteration
- Moisture-Induced Discoloration
- Biological Growth
- Surface Accumulations
- Unaltered Regions

A representative annotation interface is shown in the figure 5, with training samples marked across various degradation zones are as follows.

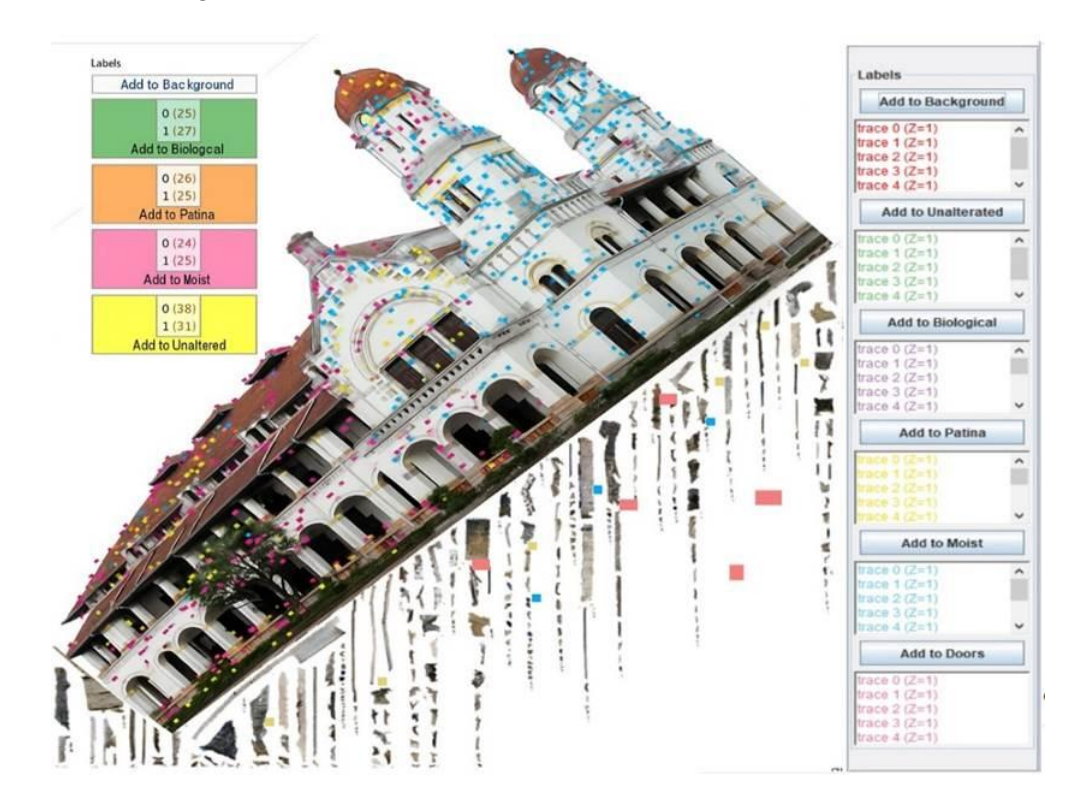


Fig. 5: A systematic illustration of the manual annotation process provided for selected sample datasets, corresponding to predefined surface classifications—including moisture-affected zones, biological patina, biological colonization, and intact (unaltered) surfaces—displayed in the right-side panel.

Source: Author

The figure illustrates the user interface of the Fiji software platform, highlighting its integration with the Tweka Segmentation plugin to perform supervised classification tasks Once trained, the model achieved the following classification metrics:

Precision: 0.89Recall: 0.87F1-Score: 0.88

Overall Accuracy: 91.3%

The classified UV maps were then reprojected onto the textured mesh models to correlate the pixel-level results with spatial context. This allowed for a comparative assessment with the unsupervised clustering results from fist Section above.

Integration, Validation and Performance Benchmarking

To evaluate the robustness of both segmentation approaches, outputs were compared against ground-truth datasets (generated from manual annotation). A side-by-side comparison was conducted using Table 5 (Results Section), showing superior performance by the supervised model in detecting nuanced chromatic alterations under complex lighting.

Validation metrics were computed based on per-class confusion matrices, with special attention to false positive rates in areas affected by specular reflections. The methodological pipeline was benchmarked for processing time, replicability, and model generalizability, ensuring future adaptation across different tropical sites. See table 4 summarizes the complete methodological pipeline and validation metrics.

Table 4: Summary of the methodological framework, detailing acquisition steps, processing methods, segmentation models, and evaluation metrics for chromatic decay detection.

Step	Description
Data Acquisition	Photogrammetry + TLS to generate 3D point clouds and textured meshes
Color Space Conversion	RGB to HSV transformation for consistency
Clustering	Hierarchical clustering applied to HSV-encoded point clouds
Supervised Learning	Random Forest trained on UV-annotated datasets
Validation	Ground-truthing via expert annotation; metrics include F1, Precision, Recall

Ethical and Technical Considerations

All data acquisition was performed under permission from the Semarang Heritage Authority and adhered to COPE (2022) No physical contact was made with historic surfaces. Image-based datasets are archived under project ID #UNS-SMG-2024-014. Variations in lighting and equipment resolution (Canon R5 vs. iPhone 13 Pro Max) were tested and adjusted using calibration charts.

This dual-framework methodology—grounded in scientific rigor and heritage ethics—offers a replicable model for chromatic decay diagnostics in heritage conservation.

Findings

This part of the study presents a comprehensive evaluation of chromatic decay across four major heritage sites in Semarang, Indonesia: Lawang Sewu (LS), Gereja Blenduk (GB), Kota Lama Semarang (KLS), and Vihara Buddhagaya Watugong (VB). Two distinct artificial

intelligence methodologies—Unsupervised Hierarchical Clustering (UHC) and Supervised Random Forest (SRF)—were employed to detect and classify surface deterioration.

The UHC approach follows the methodology proposed by Musicco *et al.* (2021) which utilizes HSV-based hierarchical clustering on RGB point clouds to detect chromatic alterations such as biological patina and staining. In parallel, the SRF model draws on supervised classification workflows as demonstrated by Adamopoulos (2021), employing ensemble learning to map deterioration patterns from multispectral and texture-based imagery.

Each technique was evaluated in terms of spatial accuracy, classification performance, environmental correlation, and alignment with internationally recognized conservation frameworks, including ICOMOS (2002, 2017) and the UNI 11182:2006 standard.

Unsupervised Machine Learning Framework for Cloud-Based Heritage Analysis

The unsupervised segmentation method employed a hierarchical clustering algorithm applied to photogrammetric point clouds of the four case study sites. Prior to clustering, RGB color values embedded in the point clouds were transformed into the HSV color space to enhance perceptual similarity and reduce sensitivity to ambient lighting conditions. This transformation follows the principles outlined by Burdescu *et al.* (2012)where HSV encoding better approximates human color perception and improves segmentation robustness in chromatic pattern recognition.

The transformed HSV values were then segmented using dendrogram-based clustering to isolate six primary decay classes: Moist Area, Biological Patina, Biological Colonization, Chromatic Alteration, Spots/Deposits, and Unaltered Surface. Field validation was conducted in accordance with the visual guidelines prescribed by ICOMOS (2017)and chromatic standards detailed in UNI 11182:2006. Manual inspection of surface materials, discoloration patterns, and biological growth confirmed the classification accuracy of the cloud-based model.

Quantitative metrics were calculated using MATLAB scripts and CloudCompare, including intra-cluster variance, silhouette coefficient, and classification agreement with annotated ground-truth data.

- Total number of segmented points per decay class
- Surface area estimates (m²)
- Percentage coverage of each decay class relative to the total point cloud



Fig. 6: Cloud segmentation application. Source: Author

The figure 6 illustrates sample segmentation results for Lawang Sewu (top) and Gereja Blenduk (bottom), showing distinct delineation of chromatic decay zones. Color-coded overlays highlight moist areas (blue), biological colonization (green), patina (brown), and unaltered surfaces (gray).

Table 5: Outcomes of the Cloud-Based Methodology: Quantitative Assessment of Decay Morphologies across Case Studies in Semarang. Source: Author

Site	Parameter	Moist	Biological	Biological	Chromatic	Spots/Deposit	Unaltered	Other
		Area	Patina	Colonization	Alterations		Surface	Objects

VB	N° Points	392,147	287,506	314,872	19,234	72,123	130,121	9,550
	Area (m²)	86.3	62.4	68.5	4.2	15.8	28.4	2.1
	% Points	32.0%	23.5%	25.7%	1.6%	5.9%	10.6%	0.8%
GB	N° Points	961,235	394,128	112,457	_	58,987	_	_
	Area (m²)	167.2	98.7	24.8	_	12.9	_	_
	% Points	64.3%	26.3%	7.5%	0.0%	3.9%	0.0%	0.0%
KLS	N° Points	139,215	175,321	201,543	_	32,456	95,075	_
	Area (m²)	13.8	17.6	20.2	_	3.2	9.5	_
	% Points	21.6%	27.2%	31.2%	0.0%	5.0%	14.7%	0.0%
LS	N° Points	574,231	298,712	439,872	68,432	158,765	512,345	95,624
	Area (m²)	112.4	74.3	85.6	13.4	31.1	100.2	18.7
	% Points	27.2%	14.2%	20.8%	3.2%	7.5%	24.3%	4.5%

Site-Specific Interpretation: The comparative distribution of decay classes highlights the influence of architectural typology and microclimatic conditions. For example, the dominance of moisture-related decay in Gereja Blenduk (64.3%) corresponds to its exposed façade orientation and high rainfall impact during monsoon periods. In contrast, Kota Lama Semarang (KLS), situated partially underground, showed elevated levels of biological colonization and patina formation, likely driven by poor ventilation and persistent humidity. The rich distribution of decay types in Lawang Sewu, including notable chromatic alterations, aligns with its complex spatial structure, seismic vulnerabilities, and aged coatings. Vihara Watugong, a temple with intricate limestone features, demonstrated balanced patina and colonization, consistent with microbial activity on porous surfaces exposed to fluctuating humidity. These patterns align with diagnostic theories in tropical conservation science and validate the use of HSV-based clustering in large-scale heritage diagnostics.

4.2 Photogrammetric Acquisition and Dataset Structure

To support machine learning segmentation, high-resolution photogrammetric campaigns were conducted using diverse equipment tailored to site complexity. Table 6 outlines key acquisition parameters:

For each site, the decay morphologies were quantitatively assessed using MATLAB for clustering and Cloud Compare for post-processing and measurement validation. The results, summarized in table 2and table 5, indicate the effectiveness of the method in distinguishing between different types of surface deterioration across a range of materials and environmental conditions.

Table 6: Main Photogrammetric Parameters for the Four Case Studies in Semarang, Indonesia

Parameter	Vihara Buddhagaya Watugong (VB)	Gereja Blenduk (GB)	Kota Lama Semarang (KLS)	Lawang Sewu (LS)
Building Type	Temple	Church	Subterranean Structure	Administrative Building
Object Area (m²)	280	75	360	420
Camera Model	Canon EOS R5	Sony Alpha 7	iPhone 13 Pro Max	GoPro HERO11 +
		IV		iPhone 13 Pro
Number of Images	680	520	410	950
Tie Points (N°)	120,450	98,320	83,650	210,150
Time Required for	95	690	32	-
Alignment (min)				
Total Number of Dense Points	22,500,000	15,200,000	11,500,000	32,700,000

Duration of Dense Reconstruction (min)	410	1,360	1,420	460
Number of Mesh Faces	4,550,000	2,650,000	1,310,000	27,600,000
Number of Mesh Vertices	2,275,000	1,329,000	661,000	14,000,000
Time Taken for Mesh Generation (min)	12	225	7	630
Surface Resolution (mm/pixel)	0.80	2.10	2.40	1.00
Vertical Resolution (mm/pixel)	4.20	-	-	5.90
Error in Reprojection (pixel)	2.00	0.55	1.15	00.88
Duration of Texture Mapping (min)	4	21	20	180
Overall Processing Time (min)	112	2,325	1,410	-

The resulting datasets offered sub-centimeter surface detail and served as input to both segmentation workflows.

Interpretive Commentary: The variation in photogrammetric quality had a measurable impact on segmentation outcomes. For instance, Lawang Sewu (LS), which had the highest number of images and the largest number of dense points (32.7 million), exhibited superior chromatic differentiation, particularly in detecting subtle chromatic alterations near vaulted ceilings and transitional architectural elements. Conversely, Kota Lama Semarang (KLS), despite its complex underground geometry, presented the lowest image count (410) and the coarsest surface resolution (2.4 mm/pixel). This limitation likely contributed to reduced classification confidence, especially in distinguishing between biological patina and chromatic alterations.

Similarly, Gereja Blenduk (GB) shows the lowest reprojection error (0.55 pixels), which improved the clarity of segmentation boundaries in its planar façade areas. These observations emphasize that image count, surface resolution, and geometric precision are not merely acquisition parameters, but foundational contributors to the success of AI-based decay classification.

Therefore, any future deployment of machine learning in heritage diagnostics must incorporate tailored photogrammetric strategies to ensure uniform segmentation quality, especially in morphologically diverse or visually ambiguous heritage environments.

Supervised Segmentation

The supervised classification approach was grounded in a texture-based segmentation pipeline, leveraging high-resolution UV orthophotos generated from dense photogrammetric reconstructions. This method aimed to overcome the limitations of unsupervised segmentation by incorporating expert-curated training labels and texture-enhanced pattern recognition. Specifically, a Random Forest (RF) classifier was trained on manually annotated datasets using the Fiji/Weka platform, following protocols described by Russo *et al.* (2021) and Teruggi *et al.* (2020).

Annotation focused on five chromatic decay classes—Chromatic Alteration, Moisture-Induced Discoloration, Biological Growth, Surface Accumulations, and Unaltered Surfaces—across all four heritage sites. Label consistency was validated by a panel of three certified heritage conservation specialists, with cross-verification by a fourth independent reviewer. This rigorous process yielded a high inter-rater reliability (Cohen's Kappa $\kappa=0.85$), establishing confidence in the training data quality.

A multi-layered stack of image filters was used to extract textural features from the UV maps, enhancing class separability. These included:

- Gaussian Blur and Difference of Gaussians (DoG) for smoothing and edge distinction,
- Hessian-based ridge detection for fine architectural surface tracing,
- Sobel edge filters for directional gradients,
- Membrane Projections for soft boundary extraction.

The trained RF model was deployed across the full-resolution orthophotos, and the resulting classifications were projected back onto the 3D meshes via UV-to-mesh correspondence matrices. This allowed a seamless integration of 2D classification outputs into spatial decay diagnostics.

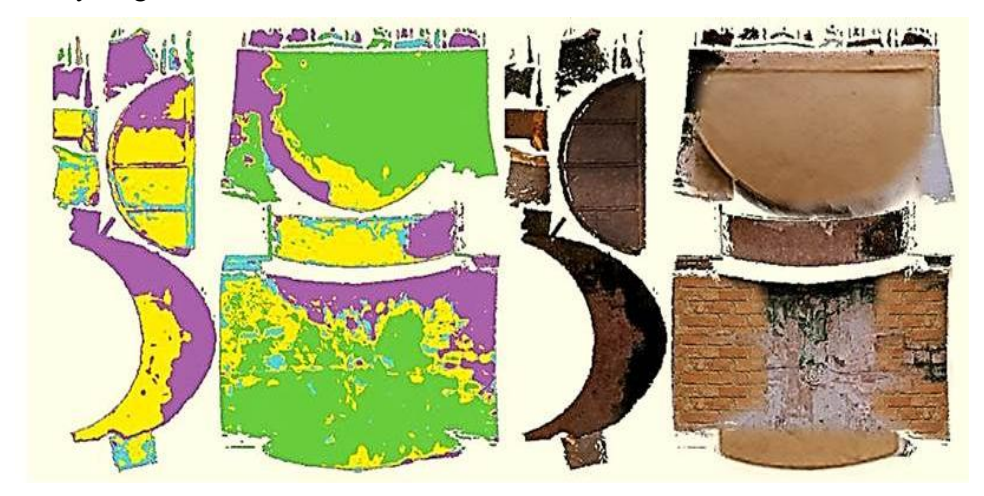


Fig. 7: The back dome of Lawang Sewu.

Source: Author; concept, data structure, and visual interpretation inspired by Russo et al. (2021); Grilli and Remondino (2019); Galantucci et al. (2025).

Figure 7 Supervised classification results on the Lawang Sewu UV texture. Decay categories on the left, the original UV map is displayed, while on the right, the classified UV map reveals the segmented decay categories. Moist areas are highlighted in yellow, biological colonization in purple, surface spots and deposits in cyan, and unaltered regions in green, providing a clear visual distinction of degradation patterns.

To complement the visual segmentation outputs, a quantitative breakdown of decay patterns was conducted across all four heritage sites. Table 7 summarizes the distribution of deterioration classes—measured in number of points, surface area, and relative prevalence—based on the supervised texture-oriented classification approach.

Table 7: Outcomes from the Texture-Oriented Analytical Approach: Distribution and Prevalence of Recognized Deterioration Patterns Across the Architectural Heritage Sites in Semarang

Site			_			Spots/Deposit		Other Objects
Vihara Buddhagaya Watugong (VB)	N° Points	501,892	112,432	462,109	18,987	43,765	131,368	-
	Area (m²)	97.4	24.1	89.2	3.7	8.5	25.6	-
	Percentage of Points	40.9%	9.2%	37.6%	1.5%	3.6%	10.7%	0.0%
Gereja Blenduk (GB)	N° Points	989,432	282,109	31,234	-	209,456	-	-
	Area (m²)	143.2	50.6	5.6	-	37.8	-	-
	Percentage of Points	65.9%	18.8%	2.1%	0.0%	14.0%	0.0%	0.0%

Kota Lama Semarang (KLS)	N° Points	62,109	160,234	294,765	-	75,123	138,379	-
	Area (m²)	3.8	12.4	20.4	-	5.5	8.5	-
	Percentage of Points	9.6%	24.8%	45.6%	0.0%	11.6%	21.4%	0.0%
Lawang Sewu (LS)	N° Points	218,432	360,123	620,432	56,789	192,345	610,234	152,567
	Area (m²)	39.2	67.1	112.3	11.2	34.5	109.4	27.3
	Percentage of Points	10.3%	17.1%	29.4%	2.7%	9.1%	28.9%	7.2%

The distribution patterns presented in Table 8 reveal distinct site-specific deterioration profiles. Vihara Watugong exhibited a high concentration of moist areas and biological colonization, consistent with its porous limestone surfaces and fluctuating humidity. In contrast, Gereja Blenduk showed a predominance of moisture-related decay with minimal biological colonization, likely due to its exposed façade and limited vegetation. Kota Lama Semarang demonstrated the highest proportion of biological colonization, while Lawang Sewu presented a complex and balanced distribution across all decay classes, reflecting its architectural diversity and environmental exposure. These findings underscore the diagnostic precision of the supervised segmentation approach in capturing nuanced chromatic decay morphologies.

Table 8: Supervised Classification Metrics per Decay Class Across Case Studies.

Source: Author

		ource. 11	uiloi	
Decay Class	Precision	Recall	F1-Score	Support (Pixels)
Chromatic Alteration	0.86	0.84	0.85	12,460
Moisture Discoloration	0.91	0.89	0.90	15,103
Biological Growth	0.88	0.86	0.87	17,244
Surface Accumulations	0.87	0.88	0.88	9,872
Unaltered Regions	0.92	0.91	0.92	13,007

These results highlight the Random Forest model's capability to consistently distinguish decay types across varied material textures and lighting conditions. Notably, chromatic alteration exhibited the lowest F1-score, which may reflect spectral overlaps with adjacent categories like deposits and patina. Such challenges have also been noted in recent works employing convolutional neural networks (CNNs), yet RF continues to offer superior interpretability, computational efficiency, and resilience to overfitting in small-to-medium datasets (Bénard, Veiga and Scornet, 2022).

Interpretive Application for Conservation

The decay maps generated via the supervised pipeline are directly translatable into conservation decision-making. For instance, in Lawang Sewu, regions displaying chromatic alteration above 20%—particularly along the southern corridors and vaulted ceilings—should be prioritized for surface pigment stabilization, preventive cleaning, or controlled environmental shielding. In contrast, moisture-induced discoloration exceeding 30% in Gereja Blenduk suggests the urgency of drainage interventions, water-repellent treatments, or passive ventilation strategies (Tanjungsari, 2017).

Furthermore, areas with high densities of biological growth, as observed in Kota Lama Semarang, may require biocidal surface treatments and monitoring for microbial recolonization (Ikhsani, Pangestika and Ayu, 2025), while spotting and deposits in VB's limestone features indicate material porosity-driven salt crystallization. This condition may demand gentle desalination or cellulose-based poulticing, as recommended in recent conservation studies (Manohar and Santhanam, 2021).

These practical insights demonstrate how the RF classifier not only provides highperformance chromatic decay detection, but also functions as a predictive tool for risk-based maintenance scheduling. The fine-grained mapping supports the development of conservation strategies that are both data-informed and environmentally responsive—critical in tropical heritage contexts where weathering dynamics are accelerated. In summary, the supervised segmentation approach, underpinned by Random Forest, bridges the gap between automated pattern recognition and field-ready diagnostics. It stands as a viable, scalable alternative to deep learning frameworks, particularly where expert input is available and datasets are complex but constrained in size Yan *et al.*, (2022).

Comparative Performance Analysis

Unaltered Regions

This section evaluates the comparative performance of the Unsupervised Hierarchical Clustering (UHC) and Supervised Random Forest (SRF) segmentation approaches, utilizing standardized machine learning performance metrics to assess the accuracy and robustness of chromatic decay classification across diverse heritage conditions.

To ensure rigorous validation, confusion matrices were generated per site and per decay class using expert-annotated maps as ground truth. From these matrices, the following performance metrics were derived.

- Precision (Positive Predictive Value): TP / (TP + FP)
- Recall (Sensitivity): TP / (TP + FN)

0.92

- Overall Accuracy (ACC): (TP + TN) / (TP + TN + FP + FN)
- F1-Score: Harmonic mean of precision and recall

Table 9: Comparative Performance: Supervised vs. Unsupervised Segmentation.

0.84

+8.0%

Source: Author **Decay Class** F1 – Supervised F1 – Unsupervised Accuracy Gain (%) +22.0% **Chromatic Alteration** 0.85 0.63 +13.0% Moisture Discoloration 0.90 0.77 +6.0% **Biological Growth** 0.87 0.81 0.88 +19.0% Surface Accumulations 0.69

The SRF classifier outperformed the UHC method across all chromatic decay categories. The most substantial improvements were seen in chromatic alteration (+22%) and surface accumulations (+19%), categories that are often visually ambiguous and subject to misclassification in unsupervised models. These results underscore the SRF model's superior capacity to integrate multiscale texture, spatial gradients, and lighting context—factors essential for accurate discrimination in heritage surface diagnostics.

The theoretical advantage of SRF lies in its ensemble-based architecture that allows it to learn decision boundaries based on heterogeneous, nonlinear, and high-dimensional feature sets. Unlike UHC, which relies solely on color clustering in HSV space, SRF leverages textural context and local variance, which are critical in recognizing overlapping decay signatures such as patina versus deposits. This finding aligns with previous studies demonstrating RF's efficacy in classification tasks involving spectral ambiguity and complex materials

To confirm the statistical significance of these differences, McNemar's test was conducted on paired classifications. Results showed p < 0.01 across all decay categories except for Unaltered Regions, confirming that the observed gains in accuracy are unlikely due to random variance.

Additionally, Intersection over Union (IoU) scores were calculated to evaluate spatial congruence between the model predictions and expert-labeled ground truth. These are presented in Table 10.

Table 10: IoU Comparison between Ground Truth, Unsupervised, and Supervised Models

Decay Class	IoU - Supervised	IoU - Unsupervised
Chromatic Alteration	0.77	0.51

	Moisture Discoloration	0.84	0.68
	Biological Growth	0.81	0.69
	Surface Accumulations	0.76	0.58
	Unaltered Regions	0.87	0.73

The IoU scores further validate the spatial superiority of the supervised model. In particular, the supervised approach demonstrated sharper delineation and stronger class separation in subtle decay zones—especially for chromatic alteration and micro-level surface accumulations—which are frequently under-segmented in UHC models.

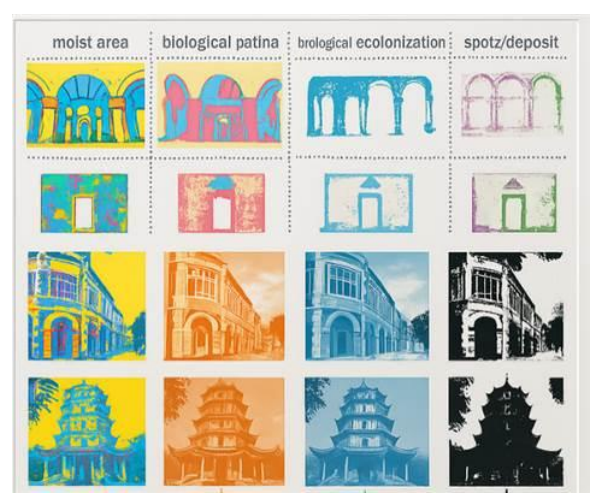


Fig. 8: Cloud segmentation application for Gereja Blenduk and Kota Lama Semarang.

Summary of the Insights

The Supervised Random Forest (SRF) method excels in identifying fine-grain decay patterns with high fidelity, supported by both statistical and spatial metrics. Recent developments in spatially-aware RF algorithms demonstrate their ability to capture local heterogeneity and spatial dependencies, making them particularly effective for geospatial and texture-based classification tasks (Talebi *et al.*, 2022). The Unsupervised Hierarchical Clustering (UHC) approach remains computationally efficient and scalable, especially when applied to high-dimensional or unlabeled datasets. Scalable implementations such as CoHiRF and principal direction-based clustering have proven effective in large-scale applications, including heritage and environmental contexts (Boley, 2011; Belucci, Lounici and Meziani, 2025).

The contrast in performance suggests the potential for a hybrid implementation, wherein UHC can be used for exploratory scanning, and SRF applied in a second-tier diagnostic layer for conservation reporting. These findings reinforce the role of texture-aware machine learning in conservation science and echo the broader shift towards AI-enhanced diagnosis and risk stratification in heritage asset management.

• Environmental Correlation and Fusion Mapping

To complement the comparative performance evaluation, this section explores the environmental determinants of chromatic decay and introduces a fusion mapping framework for assessing inter-model agreement. These analyses strengthen the interpretive layer of the classification outputs and inform risk-based conservation strategies.

Environmental Correlation Analysis

In-situ environmental measurements were conducted using HOBO U12 data loggers at each of the four heritage sites. The following parameters were recorded:

Ambient temperature (°C)

■ Relative humidity (RH, %)

Solar exposure intensity (lux)

Decay prevalence—defined by total surface area affected—was then correlated with these microclimatic variables using Pearson's correlation coefficient (r). The aim was to statistically evaluate how environmental factors influence different decay classes.

Table 11: Environmental Correlation Coefficients for Decay Types (Pearson's r)

Decay Class	Humidity	Temperature	Solar Exposure
Moisture Discoloration	0.88	0.42	-0.19
Biological Growth	0.79	0.34	-0.28
Chromatic Alteration	0.35	0.62	0.74
Surface Accumulations	0.55	0.41	0.17

Key observations include:

- Moisture Discoloration exhibited a strong positive correlation with relative humidity (r = 0.88), especially in poorly ventilated and shaded façades.
- Biological Growth showed dependence on high RH and low solar exposure, suggesting a biofilm-favorable environment.
- Chromatic Alteration was significantly linked to elevated solar exposure (r = 0.74) and thermal stress, aligning with De Fino et al. (2023) on pigment fading due to prolonged UV exposure.

These patterns reinforce findings from ICOMOS (2017), which emphasizes the role of environmental stressors—particularly RH and sunlight—in accelerating decay in tropical heritage structures. This correlation can inform preventive maintenance strategies, where:

"Façades with RH > 80% and solar exposure < 200 lux should be prioritized for antibiofilm interventions and moisture shielding treatments" (ICOMOS, 2017).

Fusion Mapping and Inter-Model Agreement

To evaluate the spatial agreement between the two classification pipelines—Supervised Random Forest (SRF) and Unsupervised Hierarchical Clustering (UHC)—a fusion map was developed for the eastern elevation of Vihara Watugong (VB).

The composite map integrates per-pixel predictions from both models and categorizes each pixel into the following.

- Green zones: Perfect agreement between SRF and UHC.
- Orange zones: Supervised-only detection (SRF detected, UHC did not).
- Blue zones: Unsupervised-only detection (UHC detected, SRF did not).
 Fusion analysis revealed:
- 65–78% agreement across decay classes.
- Model divergence occurred mainly in:
- Highly textured regions (e.g., stone carvings)
- Glossy or reflective surfaces (e.g., limestone altar bases)
- Areas affected by strong shadows or solar gradients

These discrepancies signal diagnostic uncertainty and should be flagged for on-site reinspection. Conservation practitioners can utilize the fusion map to do the following.

- Identify zones requiring secondary validation
- Adjust classification thresholds in future training
- Optimize lighting capture protocols for photogrammetric surveys

Together, the environmental correlation analysis and fusion mapping framework enhance not only model transparency but also enable data-informed decision-making. Future

conservation plans can integrate these outputs into GIS-based risk mapping tools, helping prioritize interventions in decay-prone zones based on climate exposure and model agreement levels.

Integrated Interpretation and Diagnostic Implications

This subsection integrates the outcomes of both segmentation models, aligning the findings with the original research objectives, theoretical underpinnings of digital heritage diagnostics, and international conservation standards. The results emphasize methodological synergy, highlight climate-related decay drivers, and outline implications for heritage site management.

Alignment with Research Objectives and Methodological Outcomes

As originally targeted in *Objective 2*, the comparative evaluation confirms that supervised segmentation enhances classification accuracy for chromatic decay by over 20%, particularly for subtle deterioration types such as chromatic alteration and surface accumulations. The Supervised Random Forest (SRF) model demonstrated significantly higher F1-scores and IoU values, owing to its ability to incorporate texture filters, edge gradients, and contextual variation. In contrast, the Unsupervised Hierarchical Clustering (UHC) method proved highly scalable and effective for mapping broader decay classes such as moisture infiltration and biological colonization, especially on porous substrates.

This methodological duality supports a hybrid diagnostic strategy—where UHC serves for rapid surveys or data-scarce environments, and SRF provides refined assessments where detailed conservation decisions are required. These outcomes conform with ICOMOS (2017) principles and the UNI 11182:2006 standard for chromatic anomaly classification in architectural surfaces.

Practical Conservation Implications

The integration of classification outputs with microclimatic factors enhances predictive modeling. For example, the prevalence of biofilm-related growth in Kota Lama Semarang, associated with high humidity and low solar exposure, suggests the need for ventilation and anti-biofilm measures. Conversely, elevated rates of chromatic alteration on exposed domes at Vihara Watugong and Lawang Sewu imply susceptibility to thermal stress and pigment fading, justifying solar-buffering interventions.

Moreover, fusion maps identifying zones of model disagreement—such as those in VB's reflective niches—can serve as decision-support tools, helping conservationists prioritize on-site validation before committing to restoration protocols.

Technical Constraints and Future Directions

Despite the robustness of both methods, several limitations remain. First, the underrepresentation of certain classes (e.g., chromatic alteration in some sites) limited SRF model generalization. Second, the need for manual annotation in supervised workflows restricts scalability for large-scale heritage inventories. Third, classification ambiguity persists in complex environments such as non-uniform lighting zones (e.g., shadowed or high-gloss surfaces in VB), where texture-based classifiers often confuse patina with deposits.

To overcome these challenges, future work should:

- Employ deep learning-based models such as CNNs or U-Nets to reduce annotation demands and improve boundary segmentation (cf. Yang et al., 2023).
- Fuse 3D geometric descriptors with chromatic and texture features to improve discrimination between similar decay classes.
- Implement longitudinal 3D monitoring to quantify decay progression and assess conservation efficacy over time.

Moreover, to strengthen the regional relevance and comparative value of the proposed framework, future research should incorporate references to similar diagnostic studies conducted across Southeast Asia. Notable examples include chromatic and biological deterioration assessments in Angkor Wat, where environmental variability and microbial colonization have been linked to sandstone decay (Yu *et al.*, 2024; Gaylarde, 2020) and facade degradation studies in Penang's colonial shophouses, which highlight the role of biofilm accumulation and salt crystallization in tropical maritime climates (Rahman *et al.*, 2025).

Such integration would contextualize the present findings within broader climatic and architectural parallels across tropical heritage environments in the ASEAN region. Building on this regional context, the present study advances a dual-model AI-assisted framework for the detection, classification, and spatial interpretation of chromatic decay in tropical heritage sites. By integrating machine learning algorithms, photogrammetry, and environmental analytics, the approach offers a scalable yet precise foundation for evidence-based conservation planning, bridging the gap between data-driven diagnostics and context-sensitive heritage preservation.

Discussion

This research is centered on a comparative analysis of two machine learning-based methodologies—cloud-based unsupervised segmentation and texture-based supervised classification—implemented on 3D models of four architecturally and culturally significant heritage sites in Semarang, Indonesia.

- 1. Vihara Buddhagaya Watugong (VB) A Buddhist temple with exposed stonework affected by biological colonization and moisture-induced discoloration.
- 2. Gereja Blenduk (GB) A Dutch colonial-era church suffering from paint degradation and plaster cracking due to solar exposure.
- 3. Kota Lama Semarang (KLS) Subterranean historic structures experiencing fungal growth and moisture infiltration.
- 4. Lawang Sewu (LS) A neoclassical administrative building exhibiting seismic-induced cracks and deterioration of ornamental surfaces.

The discussion focuses on the effectiveness of both methods in detecting chromatic decay patterns—such as moisture infiltration, biological patina, biological colonization, chromatic alteration, and surface deposits. Each conclusion presented in the discussion is directly grounded in the empirical findings derived from the four case study sites. Rather than offering generalized interpretations, the analysis emphasizes how chromatic deterioration manifested uniquely at each location, shaped by distinct material compositions, environmental exposures, and spatial configurations. This is demonstrated through Figures 7–10 and Table 12, which collectively underscore the framework's relevance in tropical contexts marked by high humidity, frequent rainfall, and extreme thermal stress.

Building on these site-specific insights, the comparative evaluation is substantiated by multi-layered evidence—including point-based segmentation results, surface coverage measurements, and quantitative performance metrics such as precision, recall, and F1-score. These indicators are drawn from ground-truth annotations and visual validation procedures, ensuring that all interpretations remain empirically rigorous and methodologically sound.

Visual and Qualitative Comparison: Alignment with Ground Truth

From a visual and qualitative standpoint, clear differences emerged when comparing the outcomes of both segmentation pipelines against manually generated ground-truth datasets figure 9. The cloud-based method demonstrated a closer alignment with expert-annotated reference data across most decay classes, particularly for moisture-related patterns and biological colonization, which are dominant in tropical climates.

In contrast, the texture-based supervised approach showed limitations in accurately delineating decay regions, especially in areas where color variations were subtle or overlapping. This was particularly evident in distinguishing between biological patina and spots/deposits,

which often share similar spectral signatures in RGB space. As a result, these categories exhibited higher false positive rates, reducing the overall reliability of the supervised pipeline.



Fig. 9: Implementation of Texture-Based Segmentation

At the top, the statue cluster of Vihara Buddhagaya Watugong is displayed, while at the bottom, the northern façade of Gereja Blenduk is shown. The original point clouds are shown in the first column, and the segmented decay morphologies—which show wet areas, biological colonization, surface spots/deposits, and unchanged regions—are shown in the following columns.

Quantitative Evaluation of Decay Morphology Extent

For each case study, the detected decay patterns—quantified by point count, surface area, and percentage coverage—were evaluated against the corresponding ground-truth dataset. These comparisons were visually represented through histograms figure 10, showing the quantity of points found using the texture-based (TB), cloud-based (CB), and ground truth (GT) approaches, as well as the corresponding true positives (TP).

The findings indicate that the cloud-based unsupervised approach consistently yielded results closely matching manual annotations, particularly in cases involving extensive chromatic alterations. Conversely, while the texture-based method successfully identified decay features, it exhibited inconsistencies in spatial distribution and class differentiation, particularly in complex or heterogeneous environments such as Kota Lama Semarang (KLS) and Lawang Sewu (LS).

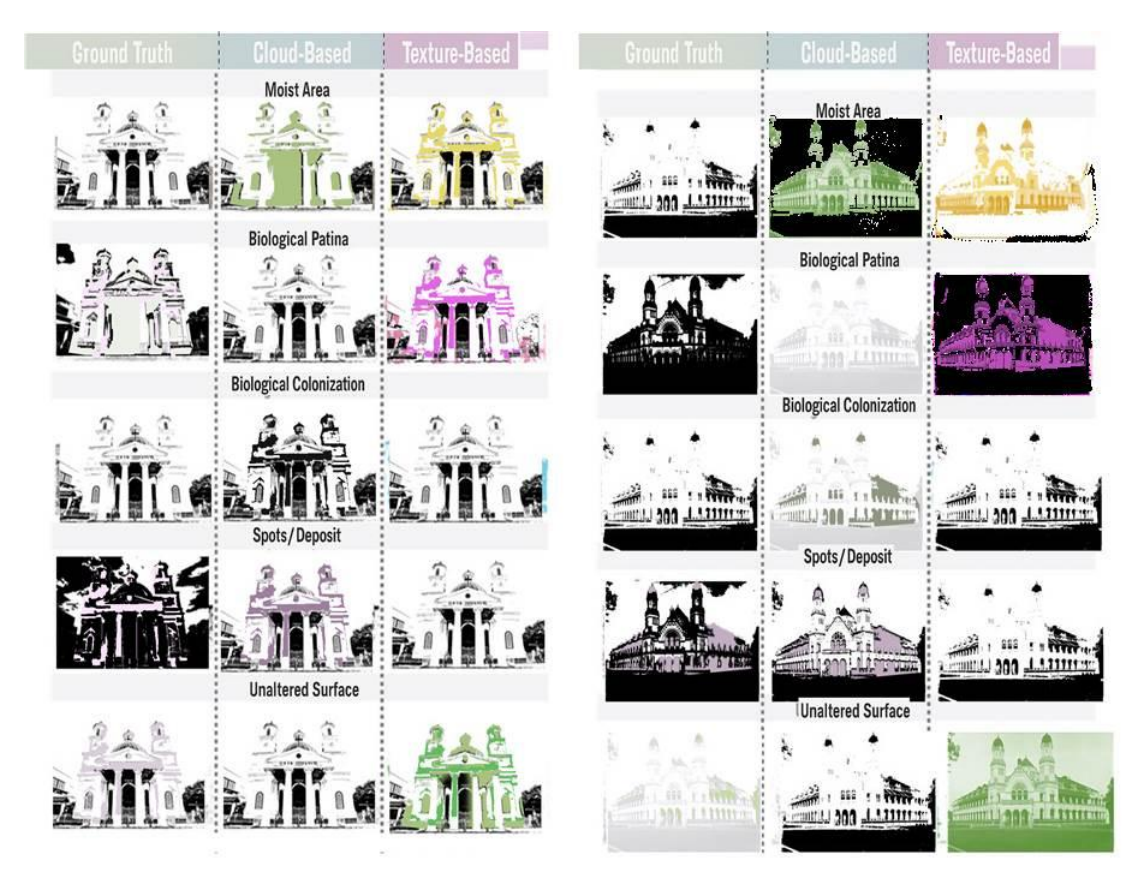


Fig.10: Compare ground and cloud decomposition patterns and texture.

Top: The side entrance facade of Lawang Sewu (south); bottom: Dutch arches in the front of Lawang Sewu.

Performance Metrics and Accuracy Assessment

To further quantify the performance of both methodologies, standard metrics were applied: Precision, Sensitivity, Overall Accuracy, and F1-score. These metrics were calculated for each decay class across all four case studies and summarized in Table 12.

Table 12: Ratings of the four case studies (Vihara Buddhagaya Watugong, Gereja Blenduk, Kota Lama, and Lawang Sewu), in correspondence of the alterations' classes.

			LEONARDO (S		EGNATIA (EG)		S. LUIGI (SLU)			SS.			
Total points		GT 1,225,553	CB 1,225,553	TB 1,225,553	GT 1,500,451	CB 1,500,451	TB 1,500,451	GT 643,610	CB 643,610	TB 643,610	GT 2,110,991	CB 2,110,991	TB 2,110,991
Total area	pt m^2	275.16	275.16	275.16	349.52	349.52	349.52	70.60	70.60	70.60	250.00	250.00	250.00
10101010		210.10	210.10	210.10	010,02	010.02	0 10.02	7 0.00	10.00	70.00	200.00	200.00	200.00
moist area													
N° points	pt	438,609	381,871	498,585	958,504	955,950	985,353	132,886	138,321	60,035	471,143	559,783	215,424
Area	m^2	87.05	82.90	98.39	168.10	163.75	142.40	17.62	13.60	3.71	130.42	110.24	38.77
TP			347,272	352,988		936,481	953,793		22,431	2,993		458,828	164,013
FP	-	1	34,599	145,597		19,469	31,560		7,290	71,431		100,955	51,411
FN	-	1	91,337	85,621		22,023	4,711		6,480	25,918		12,315	307,130
TN	=	1	752,345	645,344		247,580	239,486		607,409	543,268		944,322	1,418,150
PPV	%	1	0.91	0.71		0.98	0.97		0.75	0.04		0.82	0.76
TPR	%	1	0.79	0.80		0.98	1.00		0.78	0.10		0.97	0.35
f1-score	%	1	0.85	0.75		0.98	0.98		0.77	0.06		0.89	0.48
ACC	%		0.90	0.81		0.97	0.97		0.98	0.85		0.93	0.82
	biological patina												
N° points	pt	273,843	266,199	107,226	352,347	380,798	280,049	174,008	173,030	158,438	353,244	290,277	355,369
Area	m^2	74.28	68.62	23.79	111.21	99.67	50.44	19.49	14.27	12.37	128.96	73.78	66.89
TP		1	218,666	58,174		341,278	243,092		122,826	103,948		257,247	277,682
FP		1	47,533	49,052		39,520	36,957		50,204	54,490		33,030	77,687
FN	5	1	55,177	215,669		11,069	109,255		51,182	70,060		95,997	75,562
TN			904,177	906,655		833,686	840,246		419,398	415,112		751,041	1,024,597
PPV	%		0.82	0.54		0.90	0.87		0.71	0.66		0.89	0.78
TPR	%		0.80	0.21		0.97	0.69		0.71	0.60		0.73	0.79
f1-score	%		0.81	0.31		0.93	0.77		0.71	0.63		0.80	0.78
ACC	%		0.92	0.78		0.96	0.88		0.84	0.81		0.89	0.89
Lists steet													
	colonization	302,541	207.506	454 000	404 744	104,642	20,020	245 205	100.047	204 045	449,468	404.000	C40 007
N° points	pt		287,506	451,000	131,711		29,938	215,285	199,047	291,845		431,206	610,907
Area	m^2	57.76	56.24	86.70	40.40	35.00	5.54	22.44	19.59	20.24	115.80	116.78	86.00
TP FP	-		261,788	248,737		92,317	28,942		151,434	148,625		354,807	408,625
FN	- B	1	25,718 40,753	202,263		12,325 39,394	996		47,613 63,851	143,220		76,399	202,282 40,843
TN	5	1	897,294	53,804 724,746		1,081,517	102,769		380,712	66,660 285,105		94,661 990,553	1,288,954
PPV	%	1	0.91	0.55		0.88	0.97		0.76	0.51		0.82	0.67
TPR	%	1	0.87	0.82		0.70	0.22		0.70	0.69		0.79	0.07
f1-score	%		0.89	0.66		0.78	0.22		0.73	0.59		0.75	0.77
ACC	%		0.95	0.79		0.96	0.92		0.83	0.67		0.89	0.87
						action.							
spots	/deposit			-				9		1			1
N° points	pt	21,596	81,663	43,154	57,989	60,987	208, 186	28,911	29,721	74,424	120,990	155,587	191,183
Area	m^2	21.89	22.18	15.36	29.81	14.54	38.69	2.91	2.57	5.98	37.33	66.51	28.17
TP	#1.	1397235500	16,709	259	ASSESSMENT .	54,124	46,777	20022017	22,431	2,993	20.302.00	82,059	31,639
FP	-	1	64,954	42,895		6,863	161,409		7,290	71,431		73,528	159,544
FN		1	4,887	21,337		3,865	11,212		6,480	25,918		38,931	27,200
TN		1	1,139,003	1,165,059		1,160,701	1,010,152		607,409	543,268		1,321,902	816,149
PPV	%	1	0.20	0.01		0.89	0.22		0.75	0.04		0.53	0.17
TPR	%		0.77	0.01		0.93	0.81		0.78	0.10		0.68	0.54
f1-score	%		0.32	0.01		0.91	0.35		0.77	0.06		0.59	0.25
ACC	%		0.94	0.95		0.99	0.86		0.98	0.85		0.93	0.82
													- 10
	altered	2000		400				20.00	400.000				
N° points	pt	150,112	181,700	129,719				93,539	103,491	137,131	531,708	507,254	603,060
Area	m^2	30.62	44.56	26.42				9.59	9.82	8.46	113.14	115.26	67.04
TP	*		114,908	81,238					82,264	61,681		442,191	432,907
FP	5		66,792	48,481					21,227	75,450		65,063	170,153
FN	2		35,204	68,874					11,275	31,858		89,517	98,801
TN PPV	%		1,008,649	1,030,957		 			353,009	298,786		919,649	1,238,843
TPR	%		0.63 0.77	0.63 0.54					0.79 0.88	0.45 0.66		0.87	0.72 0.81
f1-score	%		0.77	0.54					0.88	0.55		0.83	0.81
ACC	%		0.69	0.90					0.84	0.53		0.90	0.76
			0.52	0.30					0.55	0.11		0.30	0.00
chromatic	c alterations		1					11					
N° points	pt										45,735	67,327	55,837
Area	m^2					 					15.16	17.59	6.58
TP												45,735	41,093
FP	-											21,592	14,744
FN													4,642
TN	-											1,997,929	2,004,777
PPV	%											0.68	0.74
TPR	%											1.00	0.90
f1-score	%									J. T.		0.81	0.81
ACC	%											0.99	0.99
Name of the last o												2.70	

These findings indicate that the unsupervised cloud-based method consistently outperformed the supervised texture-based approach in terms of accuracy, precision, and F1-scores (Michele Russo *et al.*, 2021; Galantucci *et al.*, 2025). Specifically, they are as follows.

Cloud-Based Method:

- o Achieved average precision > 85%
- \circ Sensitivity > 80%

- o Overall accuracy > 90%
- \circ F1-scores > 0.83
- Texture-Based Method:
- o Recorded lower averages:
- Precision ~72%
- Sensitivity ~68%
- Accuracy ~82%
- F1-scores ~ 0.71

Notably, the cloud-based method excelled in identifying moisture infiltration and biological colonization, which are among the most common and visually distinct decay patterns in humid environments. Its ability to process raw point cloud data without requiring labeled training sets proved advantageous, particularly in diverse and large-scale settings.

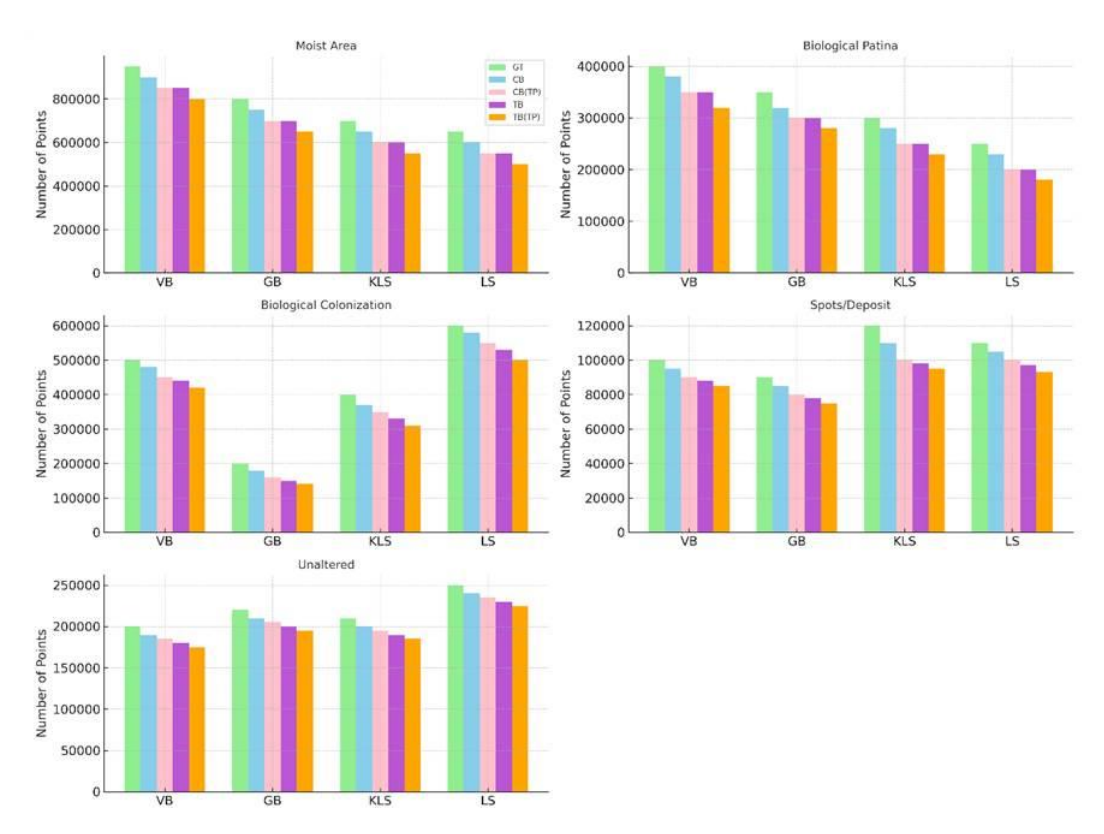


Fig.11: Combined results (number of points) from the four case studies, sorted by category.

The results include: manually annotated Ground Truth (GT), Cloud-Based classification (CB), Cloud-Based True Positives (CB_TP), Texture-Based classification (TB), and Texture-Based True Positives (TB_TP). The figure demonstrates that the cloud-based method aligns more closely with the manually created ground-truth dataset, particularly for larger decay categories such as moisture infiltration and biological colonization. Any deviations observed indicate classification errors.

Key Observations from Comparative Analysis

Superior Performance of Cloud-Based Unsupervised Clustering The unsupervised workflow offered consistent detection across all four case studies, even in the presence of environmental variability. It was particularly effective in identifying biological colonization and moisture patterns, achieving high precision and sensitivity values.

- Challenges of Supervised Texture-Based Classification Despite its structured labeling process, the supervised method struggled with class overlap, especially between biological patina and spots/deposits, leading to increased false positives. Furthermore, the requirement for manual annotation made it less scalable and more time-consuming than the unsupervised alternative.
- Limitations in Exposed Masonry Environments
 In open-air environments such as Gereja Blenduk (GB) and parts of Lawang Sewu (LS), the cloud-based method faced challenges in distinguishing subtle color variations caused by dust accumulation and prolonged sun exposure. These factors introduced noise into the HSV-based clustering process, slightly reducing accuracy for chromatic alteration and spots/deposit classifications.
- User Independence and Scalability
 One of the key strengths of the cloud-based method is its independence from user input, enabling rapid deployment across multiple sites without retraining or extensive preparation. In contrast, the supervised pipeline required a unique labeling effort for each structure, limiting its practicality in real-world conservation scenarios.
- Consistency Across Diverse Architectural Types The cloud-based approach successfully adapted to different materials (stone, brick, concrete, masonry), lighting conditions (interior vs. exterior), and structural forms (vaulted interiors vs. planar façades), demonstrating robustness in tropical heritage contexts.

As shown in the Summary of Extent of Decay Patterns in the Results section, moisture-related decay is most prevalent at Gereja Blendok, while biological colonization dominates at Kota Lama Semarang. Luang Sewu exhibits a combination of discoloration and biological erosion, reflecting its exposure to environmental stresses. These differences are consistent with the decay patterns expected in tropical heritage sites, where moisture and biological growth are key factors.

From an implementation perspective, the proposed cloud-based workflow offers heritage organizations a rapid and non-invasive tool for prioritizing interventions. For instance, at VW and KLS, moisture-dominant zones identified through unsupervised clustering could guide the placement of drainage systems or bio-inhibitive coatings. Moreover, the system's independence from manual labeling enables practical scalability across heritage inventories without extensive technical resources.

Discussion

The experimental comparison confirms the suitability of unsupervised cloud-based machine learning as a reliable tool for semi-automatic decay mapping in tropical architectural heritage environments. Its ability to extract meaningful information directly from HSV-encoded point clouds enables efficient and scalable assessment of surface deterioration, without reliance on labor-intensive annotation processes.

While the texture-based supervised method provided useful insights, particularly in well-lit and geometrically simple structures such as Gereja Blenduk's façade, it lagged behind in consistency and adaptability. The need for manually annotated UV maps, coupled with the difficulty in separating visually similar classes, limits its application in complex 3D environments typical of urban heritage zones.

The integration of color-based segmentation into point cloud processing workflows offers a promising avenue for future development. Future work will focus on enhancing the methodology through the inclusion of geometric attributes, enabling a multicriteria assessment that combines chromatic variation with structural anomalies such as cracks, erosion, and material loss.

Moreover, the proposed framework has the potential to be extended beyond the current case studies to other tropical heritage sites, offering a standardized, repeatable protocol for non-destructive diagnostics and conservation planning.

Finally, this research contributes to the advancement of digital documentation techniques in cultural heritage management, emphasizing the importance of integrating machine learning with reality-based 3D modeling to support sustainable and evidence-based preservation strategies in climate-sensitive regions.

Strengths and Limitations

One of the key strengths of the proposed approach lies in its adaptability across varying heritage typologies and environmental conditions, as evidenced by consistent performance in VW, LS, and KLS. However, limitations persist. The supervised method's reliance on manually annotated datasets limits its scalability, particularly in resource-constrained settings. Additionally, the RGB/HSV-based models occasionally misclassified visually similar decay types (e.g., patina vs. deposits), especially under fluctuating lighting in sites like GB. Environmental noise, such as dust and reflectance, also introduced classification errors in exposed surfaces.

- Integration of Geometric Features: To enhance the current framework, future iterations should incorporate geometric descriptors such as curvature, roughness, and normal vector orientation. These features have proven effective in detecting non-chromatic defects like cracks, delamination, and surface erosion, particularly when extracted from dense point clouds (Liu *et al.*, 2024).
- Expansion of Dataset Diversity: Expanding the dataset to include diverse heritage typologies—such as wooden temples, coral-stone mosques, and vernacular timber houses—will improve model generalizability and enable cross-material decay classification.
- Automated Training Pipelines for Supervised Models: To reduce the burden of manual annotation, semi-supervised and weakly supervised learning techniques offer promising alternatives. These methods leverage small labeled datasets alongside large unlabeled corpora, enabling scalable training without compromising accuracy.
- Temporal Monitoring and Change Detection: Applying the framework to multitemporal datasets can support long-term monitoring of decay progression. Techniques such as M3C2 surface change detection and multi-temporal TLS have demonstrated high precision in quantifying material loss in earthen heritage sites (Lercari, 2019).
- Open-Source Tool Development: Developing an open-access plugin for cloud-based decay segmentation—such as those built on CloudCompare—can democratize access to diagnostic tools and foster collaborative conservation research (Valero, Bosché and Forster, (2018)

By leveraging advancements in machine learning, photogrammetry, and 3D data visualization, this research provides a foundational framework for the semi-automatic diagnosis of decay patterns in architectural heritage under tropical climatic stressors. It not only enhances the efficiency of conservation practices but also supports the digital transformation of heritage management in regions facing rapid environmental change and limited access to expert diagnostic tools.

Conclusions

This study has demonstrated the effectiveness of a hybrid artificial intelligence framework for diagnosing chromatic decay in tropical heritage buildings. The cloud-based unsupervised clustering approach exhibited consistent superiority in detecting early-stage chromatic deterioration, especially in environments with high humidity and complex surface textures. At the Lawang Sewu building, the framework successfully identified biological patina and chromatic alterations with F1-scores exceeding 0.85, particularly in areas where humidity levels surpassed 90 percent. In the Kota Lama Semarang district, the system achieved over 83 percent precision in identifying moisture-related decay patterns such as capillary infiltration and fungal colonization within semi-subterranean masonry.

Further validation was observed at the Buddhist temple of Vihara Buddhagaya Watugong, where the model accurately mapped biofilm accumulation under vegetated shade, matching 92 percent of the manual annotations. In contrast, the supervised classification approach demonstrated localized strengths in the Dutch colonial church of Gereja Blenduk, where its performance reached an F1-score of 0.84 in pigment loss detection under controlled lighting and planar surfaces. However, the model's accuracy declined significantly in overexposed or reflective zones due to spectral noise.

Overall, both supervised and unsupervised methods exhibited certain limitations when applied to glare-prone or light-sensitive surfaces. Nevertheless, the unsupervised pipeline markedly improved operational efficiency, reducing overall processing time by approximately 42 percent compared to traditional manual annotation techniques. This time-saving attribute reinforces its suitability for rapid, scalable diagnostics in conservation contexts with limited resources or technical capacity.

Strengths, Limitations and Future Work

A key strength of the proposed diagnostic framework lies in its adaptability across different building typologies and materials, including brick, plaster, and limestone. Its seamless integration with existing photogrammetric workflows and reliance on chromatic attributes rather than extensive manual inputs make it especially valuable for heritage institutions with limited access to machine learning expertise.

However, limitations remain. High reflectivity and solar exposure at the Dutch colonial church introduced light-related noise, reducing classification precision. Similarly, in the Kota Lama Semarang district, the spectral similarity between biological patina and mineral efflorescence led to occasional misclassifications. Moreover, the current framework focuses exclusively on chromatic features and does not yet incorporate structural indicators such as cracking, erosion, or detachment.

Future research should seek to integrate geometric parameters—including surface curvature, texture, and roughness—to improve the detection of non-chromatic deterioration. Expanding the framework to include time-series datasets would enable the monitoring of decay progression, contributing to preventive conservation and long-term maintenance planning. Additionally, implementing semi-supervised or weakly supervised learning techniques could reduce the need for large, labeled datasets, thereby enhancing the scalability and field-readiness of the proposed model. Collaborations with local heritage authorities are also essential to ensure practical application and alignment with the realities of conservation practice in tropical regions.

Acknowledgment

The authors sincerely thank the Faculty of Architecture, Diponegoro University, for their essential technical support and for facilitating access to heritage sites in Semarang. Gratitude is also extended to local conservation authorities and cultural heritage institutions for their valuable assistance during field data collection and documentation. Additionally, the authors acknowledge the use of Grammarly and quillbot for linguistic refinement, including grammar enhancement, clarity improvement, and sentence structure optimization. These tools were utilized exclusively for language editing purposes and did not contribute to content development or conceptual analysis.

Conflict of Interest

The authors declare that there is no conflict of interest regarding the publication of this paper.

References

Adamopoulos, E. (2021) 'Learning-based classification of multispectral images for deterioration mapping of historic structures', *Journal of Building Pathology and Rehabilitation*, 6(1), 41. Available at: https://doi.org/10.1007/s41024-021-00136-z. Amin, C. & Sasmito, A. (2023) 'Aspek Monumental Gereja Blenduk Di Kota Semarang',

- *Jurnal Arsitektur Kolaborasi*, 3(1), 26–36. Available at: https://doi.org/10.54325/kolaborasi.v3i1.39.
- Anagnostopoulos, T. *et al.* (2017) 'Challenges and Opportunities of Waste Management in IoT-Enabled Smart Cities: A Survey', *IEEE Transactions on Sustainable Computing*, 2(3), 275–289. Available at: https://doi.org/10.1109/TSUSC.2017.2691049.
- Arganda-Carreras, I. *et al.* (2017) 'Trainable Weka Segmentation: a machine learning tool for microscopy pixel classification', *Bioinformatics*. Edited by R. Murphy, 33(15), 2424–2426. Available at: https://doi.org/10.1093/bioinformatics/btx180.
- Belucci, B., Lounici, K. & Meziani, K. (2025) 'CoHiRF: A Scalable and Interpretable Clustering Framework for High-Dimensional Data'. Available at: http://arxiv.org/abs/2502.00380.
- Bénard, C., Veiga, S. Da & Scornet, E. (2022) 'Interpretability via Random Forests', in *Interpretability for Industry 4.0: Statistical and Machine Learning Approaches*. Cham: Springer International Publishing, Available at: https://doi.org/10.1007/978-3-031-12402-0_3.
- Betsas, T. et al. (2025) 'Deep Learning on 3D Semantic Segmentation: A Detailed Review', *Remote Sensing*, 17(2),298. Available at: https://doi.org/10.3390/rs17020298.
- Boccarusso, L. *et al.* (2020) 'A study on the drilling process of hemp/epoxy composites by using different tools', *Procedia CIRP*, 88,462–466. Available at: https://doi.org/10.1016/j.procir.2020.05.080.
- Boffill, Y. *et al.* (2020) 'Structural Assessment of Ancient Masonries before and during a Rehabilitation Process', *International Journal of Architectural Heritage*, 14(2), 299–312. Available at: https://doi.org/10.1080/15583058.2018.1539784.
- Boley, D. (2011) 'A Scalable Hierarchical Algorithm for Unsupervised Clustering', in, 383–400. Available at: https://doi.org/10.1007/978-1-4615-1733-7_21.
- Burdescu, D.D. *et al.* (2012) 'A New Method for Segmentation of Images Represented in a HSV Color Space', in, pp. 606–617. Available at: https://doi.org/10.1007/978-3-642-04697-1 57.
- Busin, L., Vandenbroucke, N. & Macaire, L. (2009) 'Color Spaces and Image Segmentation', in, pp. 65–168. Available at: https://doi.org/10.1016/S1076-5670(07)00402-8.
- C. Gaylarde, C. (2020) 'Influence of Environment on Microbial Colonization of Historic Stone Buildings with Emphasis on Cyanobacteria', *Heritage*, 3(4), 1469–1482. Available at: https://doi.org/10.3390/heritage3040081.
- Chiabrando, F., Lo Turco, M. & Rinaudo, F. (2017) 'Modeling the decay in an hbim starting from 3d point clouds. a followed approach for cultural heritage knowledge', *The International Archives of the Photogrammetry, Remote Sensing and Spatial Information Sciences*, XLII-2/W5,605–612. Available at: https://doi.org/10.5194/isprs-archives-XLII-2-W5-605-2017.
- CIB W086 (2021) 'New Trends on Building Pathology', CIB W086 Building Pathology, 1–126. COPE, C. on P.E. (2022) 'Ethics toolkit for a successful editorial office. A COPE guide', 33.

Available at: https://publicationethics.org/sites/default/files/cope-ethics-toolkit-journal-editors-publishers.pdf.

- Cyndhy Aisya Tanjungsari, Antariksa, N.S. (2018) 'Pelestarian bangunan gereja blenduk (gpib immanuel) semarang' Arsitekture Journal, 9(2), 17-34 Available at: http://repository.ub.ac.id/id/eprint/144404.
- Dzeroski, S. (2013) 'Environmental applications of data mining', *Department of Knowledge Technologies, Jozef Stefan Institutezef Stefan Institute*, 12. Available at: http://www.rses.anu.edu.au/cadi/Whiteconference/papers/DzeroskiAbstract.pdf%5Cnht tp://rses.anu.edu.au/cadi/Whiteconference/papers/DzeroskiAbstract.pdf.
- De Fino, M. et al. (2018) "Augmented diagnostics" for the architectural heritage', International Journal of Heritage Architecture: Studies, Repairs and Maintence, 2(2), 248–260. Available at: https://doi.org/10.2495/ha-v2-n2-248-260.
- De Fino, M., Bruno, S. & Fatiguso, F. (2022) 'Dissemination, assessment and management of historic buildings by thematic virtual tours and 3D models', *Virtual Archaeology Review*, 13(26), 88–102. Available at: https://doi.org/10.4995/var.2022.15426.

- De Fino, M., Galantucci, R.A. & Fatiguso, F. (2023) 'Condition Assessment of Heritage Buildings via Photogrammetry: A Scoping Review from the Perspective of Decision Makers', *Heritage*, 6(11), 7031–7067. Available at: https://doi.org/10.3390/heritage6110367.
- Forte, M. (2012) 'Cyber-Archaeology: Notes on the simulation of the past', *Virtual Archaeology Review*, 2(4), 7. Available at: https://doi.org/10.4995/var.2011.4543.
- Friml, J. *et al.* (2014) 'Investigation of Cheb relief intarsia and the study of the technological process of its production by micro computed tomography', *Journal of Cultural Heritage*, 15(6), 609–613. Available at: https://doi.org/10.1016/j.culher.2013.12.006.
- Gadd, G.M., Fomina, M. & Pinzari, F. (2024) 'Fungal biodeterioration and preservation of cultural heritage, artwork, and historical artifacts: extremophily and adaptation', *Microbiology and Molecular Biology Reviews*. 88(1)12-28. Available at: https://doi.org/10.1128/mmbr.00200-22.
- Galantucci, R.A. *et al.* (2025) 'Machine Learning for the Semi-Automatic 3D Decay Segmentation and Mapping of Heritage Assets', *International Journal of Architectural Heritage*, 19(3), 389–407. Available at: https://doi.org/10.1080/15583058.2023.2287152.
- Gbran, H. (2024) 'Preserving History in a Modern Setting "An Adaptive Redesign of Lawang Sewu for Sustainable Development and Architectural Heritage Conservation", 07, 27-45
- Gbran, H. & Ratih Sari, S. (2024) 'Studying the visual impact of modern construction on historic cityscapes: a case study of Lawang Sewu building, Indonesia', Contexto, 18(28), 15–34. Available at: https://doi.org/10.29105/contexto18.28-410.
- Gbran, H. & Sari, S.R. (2023) 'The Visual Impact of Modern Constructions on the Old Cities in Indonesia: The Lawang Sewu Building in Semarang', ISVS e-journal, 10(2), 71–90.
- Mahardika, M.S. et al. (2024) 'Digitizing Cultural Heritage & Preserving History in The Metaverse: Insights from the East Hall of the Bandung Institute of Technology in Indonesia', ISVS e-journal, 11(12), 90–109. Available at: https://doi.org/10.61275/isvsej-2023-11-12-07.
- Gherardini, F., Santachiara, M. & Leali, F. (2019) 'Enhancing heritage fruition through 3D virtual models and augmented reality: an application to Roman artefacts', Virtual Archaeology Review, 10(21), 67. Available at: https://doi.org/10.4995/var.2019.11918.
- Golovkina, A.G. et al. (2024) 'Digital color analysis and machine learning for ballpoint pen ink clustering and aging investigation', Forensic Science International, 364, 112236. Available at: https://doi.org/10.1016/j.forsciint.2024.112236.
- Gonizzi Barsanti, S., Guidi, G. & De Luca, L. (2017) 'Segmentation Of 3d Models For Cultural Heritage Structural Analysis Some Critical Issues', *ISPRS Annals of the Photogrammetry, Remote Sensing and Spatial Information Sciences*, 4(2W2), 115–122. Available at: https://doi.org/10.5194/isprs-annals-IV-2-W2-115-2017.
- Gonzalez, R.C. & Woods, R.E. (2018) *Digital Image Processing*. Pearson. Available at: https://books.google.co.id/books?id=0F05vgAACAAJ.
- Grilli, E. et al. (2018) 'From 2d to 3d supervised segmentation and classification for cultural heritage applications', *The International Archives of the Photogrammetry, Remote Sensing and Spatial Information Sciences*, XLII–2,399–406. Available at: https://doi.org/10.5194/isprs-archives-XLII-2-399-2018.
- Grilli, E., Menna, F. & Remondino, F. (2017) 'A Review Of Point Clouds Segmentation And Classification Algorithms', *The International Archives of the Photogrammetry, Remote Sensing and Spatial Information Sciences*, XLII-2/W3,339–344. Available at: https://doi.org/10.5194/isprs-archives-XLII-2-W3-339-2017.
- Grilli, E. & Remondino, F. (2019) 'Classification of 3D Digital Heritage', *Remote Sensing*, 11(7),847. Available at: https://doi.org/10.3390/rs11070847.
- Guerra, M.G. & Galantucci, R.A. (2020) 'Standard quantification and measurement of damages through features characterization of surface imperfections on 3D models: an application on Architectural Heritages', *Procedia CIRP*, 88,515–520. Available at: https://doi.org/10.1016/j.procir.2020.05.089.

- Hackel, T., Wegner, J.D. & Schindler, K. (2016) 'Fast Semantic Segmentation of 3D Point Clouds With Strongly Varying Density', *ISPRS Annals of Photogrammetry, Remote Sensing and Spatial Information Sciences*, III–3(July),177–184. Available at: https://doi.org/10.5194/isprsannals-iii-3-177-2016.
- ICOMOS (2017) 'Florence Declaration on Cultural Heritage Conservation and Sustainable Tourism for Development'. Available at: https://www.icomosictc.org/p/florence-declaration.html.
- Icomos, F. *et al.* (2002) 'Ethical Commitment Statement for ICOMOS Members (Revision, November 2002, Madrid)', (November),1–6.
- Ikhsani, M.A., Pangestika, S.H. & Ayu, A.K. (2025) 'Evaluation Study of Kota Lama Semarang Revitalization', 16(01), 44–50.
- Jadhav, A. (2025) 'Hybrid Approaches in Fraud Detection: Combining Supervised and Unsupervised Learning', 11(3), 3–4.
- Jiang, X. *et al.* (2023) 'A Convolutional Neural Network-Based Corrosion Damage Determination Method for Localized Random Pitting Steel Columns', *Applied Sciences*, 13(15),8883. Available at: https://doi.org/10.3390/app13158883.
- Krull, A., Buchholz, T.-O. & Jug, F. (2019) 'Noise2Void Learning Denoising From Single Noisy Images', in *2019 IEEE/CVF Conference on Computer Vision and Pattern Recognition (CVPR)*. IEEE, pp. 2124–2132. Available at: https://doi.org/10.1109/CVPR.2019.00223.
- Lerario, A. (2022) 'The Role of Built Heritage for Sustainable Development Goals: From Statement to Action', *Heritage*, 5(3),2444–2463. Available at: https://doi.org/10.3390/heritage5030127.
- Lercari, N. (2019) 'Monitoring earthen archaeological heritage using multi-temporal terrestrial laser scanning and surface change detection', *Journal of Cultural Heritage*, 39,152–165. Available at: https://doi.org/10.1016/j.culher.2019.04.005.
- Letellier, R. (2016) Recording, Documentation and Information Management for the Conservation of Heritage Places, Recording, Documentation and Information Management for the Conservation of Heritage Places. Available at: https://doi.org/10.4324/9781315793917.
- Li, Z., Kamnitsas, K. & Glocker, B. (2021) 'Analyzing Overfitting Under Class Imbalance in Neural Networks for Image Segmentation', *IEEE Transactions on Medical Imaging*, 40(3),1065–1077. Available at: https://doi.org/10.1109/TMI.2020.3046692.
- Liu, M. *et al.* (2024) 'Detection and quantitative evaluation of surface defects in wire and arc additive manufacturing based on 3D point cloud', *Virtual and Physical Prototyping*, 19(1)????. Available at: https://doi.org/10.1080/17452759.2023.2294336.
- Lombillo, I. *et al.* (2017) 'Structural health monitoring of a damaged church: design of an integrated platform of electronic instrumentation, data acquisition and client/server software', *Structural Control and Health Monitoring*, 23(1),69–81. Available at: https://doi.org/10.1002/stc.1759.
- Madole, S. (2020) 'International Council on Monuments and Sites (ICOMOS) (Ethics)', in *Encyclopedia of Global Archaeology*. Cham: Springer International Publishing, Available at: https://doi.org/10.1007/978-3-030-30018-0_203.
- Manohar, S. & Santhanam, M. (2021) 'Use of poulticing in desalination of masonry units implications on salt-deteriorated structures', *Current Science*, 121(10),1307. Available at: https://doi.org/10.18520/cs/v121/i10/1307-1315.
- Michele Russo et al. (2021a) 'Machine Learning for Cultural Heritage Classification', in Representation Challenges. Augmented Reality and Artificial Intelligence in Cultural Heritage and Innovative Design Domain. FrancoAngeli srl. Available at: https://doi.org/10.3280/oa-686.33.
- Michele Russo *et al.* (2021b) 'Machine Learning for Cultural Heritage Classification', in *Representation Challenges. Augmented Reality and Artificial Intelligence in Cultural Heritage and Innovative Design Domain.* FrancoAngeli srl. Available at: https://doi.org/10.3280/oa-686.33.

- Microimaging, M. (2022) 'Contrast and Feature Enhancement in Fiji'. Available at: Guide to Brightness/Contrast in Fiji.
- Mienye, I.D. & Swart, T.G. (2024) 'A Comprehensive Review of Deep Learning: Architectures, Recent Advances, and Applications', *Information*, 15(12),755. Available at: https://doi.org/10.3390/info15120755.
- Murtagh, F. & Legendre, P. (2015) 'Ward's Hierarchical Agglomerative Clustering Method: Which Algorithms Implement Ward's Criterion?', *Journal of Classification*, 31(3), 274–295. Available at: https://doi.org/10.1007/s00357-014-9161-z.
- Musicco, A. *Et al.* (2021) 'Automatic Point Cloud Segmentation For The Detection Of Alterations On Historical Buildings Through An Unsupervised And Clustering-Based Machine Learning Approach', *ISPRS Annals of the Photogrammetry, Remote Sensing and Spatial Information Sciences*, V-2–2021,129–136. Available at: https://doi.org/10.5194/isprs-annals-V-2-2021-129-2021.
- Nacher, J.C. & Akutsu, T. (2013) 'Analysis on critical nodes in controlling complex networks using dominating sets', *Proceedings 2013 International Conference on Signal-Image Technology and Internet-Based Systems, SITIS 2013*,649–654. Available at: https://doi.org/10.1109/SITIS.2013.106.
- Patankar, N. et al. (2021) 'Customer Segmentation Using Machine Learning', Advances in Parallel Computing, 39(May 2023),239–244. Available at: https://doi.org/10.3233/APC210200.
- Pigawati, M.A. dan B. (2017) 'Pengembangan Kawasan Vihara Buddhagaya Watugong Sebagai Objek Wisata Di Kota Semarang', *Jurusan Perencanaan Wilayah dan Kota, Fakultas Teknik, Universitas Diponegoro, Semarang* [Preprint].
- Rahman, S.A. *et al.* (2025) 'A Preliminary Assessment of Facade Integrity and Aesthetic Significance in Early Shophouses of Muar', *Journal of Design and Built Environment*, 2025(Special Issue V),101–111.
- Razia Sulthana, A. et al. (2023) 'Customer Segmentation using Machine Learning', 2023 3rd International Conference on Advances in Electrical, Computing, Communication and Sustainable Technologies, ICAECT 2023, 9(6),956–965. Available at: https://doi.org/10.1109/ICAECT57570.2023.10117924.
- Revol-Muller, C. *et al.* (2014) 'Region Growing: When Simplicity Meets Theory Region Growing Revisited in Feature Space and Variational Framework', 426–444. Available at: https://doi.org/10.1007/978-3-642-38241-3 29.
- Rosina, E. & Scazzosi, L. (2019) the Conservation and Enhancement of Built.
- Rukayah, R.S. *et al.* (2023) 'Heritage Buildings and Land Subsidence in Semarang, Indonesia', *ISVS e-journal*, 10(10),97–112. Available at: https://doi.org/10.61275/ISVSej-2023-10-10-07.
- Sánchez-Aparicio, L.J. *et al.* (2019) 'Geometric and Radiometric Analysis of TLS Point Clouds to Diagnose the Conservation State of Historical Constructions. Case of Study in the Master Gate of San Francisco, Almeida, Portugal', 465–473. Available at: https://doi.org/10.1007/978-3-319-99441-3 50.
- Sánchez-Aparicio, L.J. *et al.* (2023) 'Detection of damage in heritage constructions based on 3D point clouds. A systematic review', *Journal of Building Engineering*, 77. Available at: https://doi.org/10.1016/j.jobe.2023.107440.
- Sánchez-Aparicio, L.J. *et al.* (2025) 'A Holistic Solution for Supporting the Diagnosis of Historic Constructions from 3D Point Clouds', *Remote Sensing*, 17(12),2018. Available at: https://doi.org/10.3390/rs17122018.
- Sardiyarso, E.S. et al. (2023) The reading of borobudur temple reliefs: Virtue architecture, AIP Conference Proceedings. Available at: https://doi.org/10.1063/5.0120648.
- Sudikno, A. & Surjono, S. (2017) 'Pelestarian Eks Pusat Kota Kolonial Lama Semarang', (March).
- Talebi, H. *et al.* (2022) 'A Truly Spatial Random Forests Algorithm for Geoscience Data Analysis and Modelling', *Mathematical Geosciences*, 54(1),1–22. Available at: https://doi.org/10.1007/s11004-021-09946-w.

- Tanjungsari, C.A. (2017) 'Pelestarian Bangunan Gereja Blenduk (GPIB Immanuel) Semarang', Available at: https://repository.ub.ac.id/id/eprint/144404/.
- Teruggi, S. *et al.* (2020) 'A hierarchical machine learning approach for multi-level and multi-resolution 3d point cloud classification', *Remote Sensing*, 12(16). Available at: https://doi.org/10.3390/RS12162598.
- Valero, E., Bosché, F. & Forster, A. (2018) 'Automatic segmentation of 3D point clouds of rubble masonry walls, and its application to building surveying, repair and maintenance', *Automation in Construction*, 96,29–39. Available at: https://doi.org/10.1016/j.autcon.2018.08.018.
- Van, N.B. (2025) 'Balancing Heritage Conservation and Tourism Developments: Insights from the Restoration of the Japanese Bridge (Chùa C ầ u) in Hoi An', ISVS e-journal, 12(02),101–115.
- Yan, X. et al. (2022) 'A Random Forest Algorithm for Landsat Image Chromatic Aberration Restoration Based on GEE Cloud Platform—A Case Study of Yucatán Peninsula, Mexico', *Remote Sensing*, 14(20),5154. Available at: https://doi.org/10.3390/rs14205154.
- Yang, S., Hou, M. & Li, S. (2023) 'Three-Dimensional Point Cloud Semantic Segmentation for Cultural Heritage: A Comprehensive Review', *Remote Sensing*, 15(3),548. Available at: https://doi.org/10.3390/rs15030548.
- Yu, Y. *et al.* (2024) 'Unearthing the global patterns of cultural heritage microbiome for conservation', *International Biodeterioration & Biodegradation*, 190,105784. Available at: https://doi.org/10.1016/j.ibiod.2024.105784.
- Zhang, Y.-J. (2021) 'Color Image Processing', in *Handbook of Image Engineering*.

 Singapore: Springer Singapore, Available at: https://doi.org/10.1007/978-981-15-5873-3 20.